SUPPLEMENTARY MATERIALS AND METHODS

Geographic Ranges of Extant Conifers

The Araucariaceae, Podocarpaceae, and Callitroideae are generally referred to as Southern Hemisphere conifers because most of their species diversity (~75%) is found south of the Equator (numbers based on midpoint species latitude ranges compiled primarily from monographs (1-4)). However, about 34% of Podocarpaceae species are found in Northern Hemisphere tropical environments (and very occasionally warm temperate forests), especially in Central America and Southeast Asia. While most species diversity in Araucariaceae and Podocarpaceae is found in southern tropical latitudes, Podocarpaceae includes a significant number of Southern temperate species (around 20% of species diversity), including a large temperate clade (the prumnopityoid clade of (5), also found in this analysis). Callitroideae are also primarily temperate, with 80% of species diversity found south of the Tropic of Capricorn. Among Northern Hemisphere conifer clades, most Pinaceae and Cupressoideae species diversity is found in mountainous temperate and warm temperate regions of western North American and southern and southwestern China. A few species of Pinaceae and Cupressoideae extend into lowland tropical environments, and only a single species of *Juniperus* (*J. procera*) extends below the Equator.

Calibration approach

In general, we did not place fossils in subclades within extant genera, because such placement often depends on the correct systematic assessment of detailed morphological features like cuticle characters or continuous variables such as the size of seed cones. Since the systematic patterns in such features have rarely been explored in an explicit phylogenetic framework, it is often difficult to confidently determine which states are pleisiomorphic and which synapomorphic. The inability to reliably assign most fossils to specific groups within modern genera, combined with relatively poor knowledge of even the most completely understood fossils, means that many fossils cannot be assigned securely to the crown group of the genus (the group that includes all living members) and could instead belong to the stem group (the group that includes all living species and some extinct species which may lack all the defining features of the living genus). We therefore conservatively place fossils as stem members unless they possess extremely distinctive morphological features shared only with particular extant clades within genera.

For all calibration points we developed an associated prior age distribution, which represents the initial probability distribution of ages for a calibrated node used in BEAST analyses. In most cases, we used priors with a lognormal probability distribution where the minimum age was set by the age of the fossil constraint and 95% confidence intervals of the probability distribution extend either 20 or 40 million years (My) earlier than this minimum age. We chose these two different distributions in order to explore the effect of prior width on divergence age estimates, although both numbers are somewhat arbitrary. In effect, we make an initial hypothesis that the actual date of a given divergence had a

95% probability of occurring within 20 or 40 My of the first fossil evidence, which can be subsequently altered by the analysis based on information from the sequence data. If fossil age is known to be within a general geologic time interval but its exact age has not been resolved, we used the younger boundary of the time period to set the minimum age. Throughout this study, dates were based on the 2009 geologic timescale published by the Geological Society of America (primarily based on 6). We used lognormal prior age distributions with either 20 or 40 My 95% confidence intervals for all calibration points unless there was fossil evidence suggesting the actual divergence may significantly predate the first unambiguous fossil appearance. For example, we extended the 95% confidence intervals beyond the typical 20 My (or 40 My in the alternate analysis) for the divergence of *Tsuga* because their seed cones first occur in the Eocene, but there are reports of their distinctive pollen grains from the Late Cretaceous (Turonian). We therefore extended the 95% confidence intervals of the prior to reflect the possibility of their earlier divergence time (see Discussion of Calibration Points and Priors for more detail). The divergence between conifers and cycads (the outgroup used in this study) was constrained between 275-350 My using a uniform prior, where any divergence age between these dates is equally probable. We used a uniform prior for this date because we are confident that the divergence did not occur before 350 My based on substantial fossil evidence, even though the relationships among putative early conifers, extant conifers, and cycads, as well as the timing of their respective appearances during this interval, have not been resolved unambiguously (see Discussion of Calibration Points and Priors).

Evaluating the Impact of Different Priors

Within the focal clades, there were only minor differences in divergence age estimates when using fossil calibrations with associated prior age distributions of 20 My or 40 My 95% confidence intervals (Table S1). Surprisingly, median node ages were slightly younger within some focal clades using the calibration scheme with wider prior age distributions. Because the differences between analyses were minimal, both in terms of absolute and relative ages, we primarily illustrate results from the analysis using 40 My prior age distributions. This analysis uses wider, more conservative prior age distributions. In this analysis, the distributions of divergence times in specific focal clades are broadly similar to overall Northern Hemisphere (NH) and Southern Hemisphere (SH) conifer distributions shown in the main text. Cupressoideae and Pinaceae distributions are skewed towards more recent divergence times than Callitroideae and Podocarpaceae, and also show proportionally fewer deep divergences (Fig. S1*A*).

Clade	**Median Node Ages (My)**		
	Observed (20 My Priors)	Observed (40 My Priors)	50% Resampling (40 My Priors)
Araucariaceae (SH)	6.13	6.07	-
Podocarpaceae (SH)	8.66	8.72	-
Podocarpus (SH)	5.67	5.96	-
Callitroideae (SH)	16.34	16.75	-
All Southern	8.45	8.72	-
Cupressoideae (NH)	4.34	4.15	4.28 (5.60) 7.82
Pinaceae (NH)	3.67	3.77	4.37 (5.04) 5.78
Pinus (NH)	3.09	3.21	3.52 (4.52) 5.09
All Northern	4.39	5.21	5.03 (5.53) 6.17

Table S1. Median node ages (in millions of years; My) of Southern Hemisphere (SH) and Northern Hemisphere (NH) focal clades using different calibration schemes. Resampled values in parentheses represent the median value of 10,000 median node ages calculated from a resampling routine where NH clades were reduced to 50% species sampling (see discussion in Supplementary Materials). Values outside of the parentheses give the lower and upper boundaries of the 95% confidence intervals for this distribution. Note that while the upper limits of the 95% confidence intervals in Cupressoideae and Pinaceae are older than observed median node age in Araucariaceae, this clade is sampled nearly as well as NH clades and its observed median node age can be directly compared with observed values in NH clades.

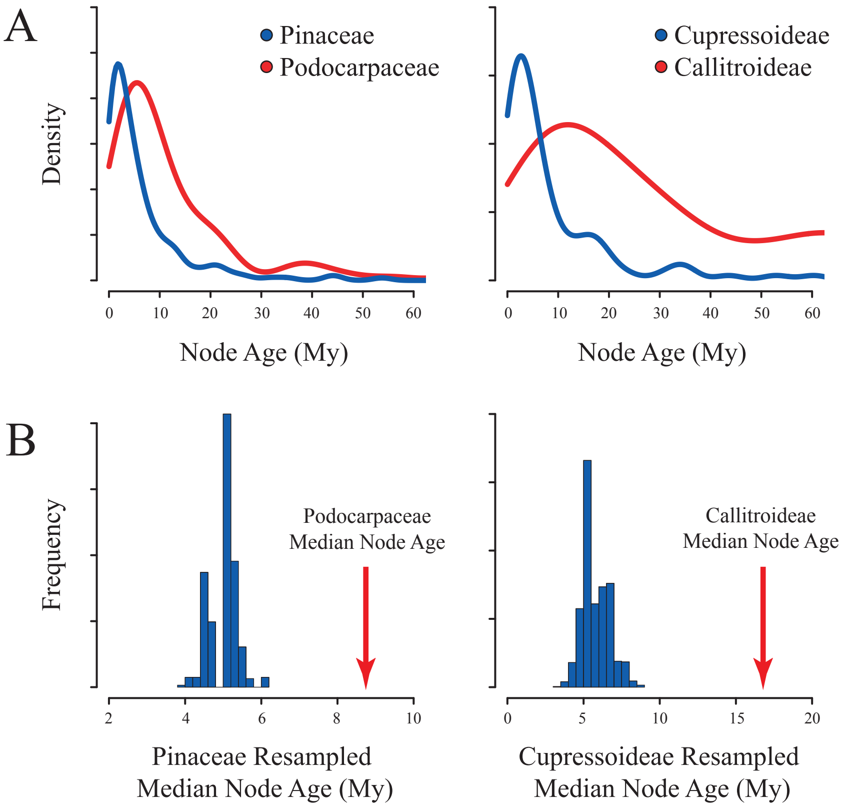

Fig. S1. (A) Distribution of divergence times (in millions of years; My) in Northern Hemisphere and Southern Hemisphere focal clades. A density function was calculated from the age distributions and then scaled to facilitate comparisons between clades with different numbers of extant species. Density values are arbitrary and are not shown on the axes. (B) Distribution of 10,000 median node ages for Pinaceae and Cupressoideae generated through an iterative resampling procedure (see discussion in Supplementary Materials). Red arrows indicate the value of the observed median node age in Podocarpaceae and Callitroideae.

Evaluating Potential Sample Bias

Southern Hemisphere clades are not as well sampled in our dataset as NH clades, which could potentially bias our results towards finding relatively older ages in SH groups. In order to assess this, we performed an iterative resampling analysis where NH clades were randomly degraded to 50% sampling of extant species and the median node age was recalculated. This was repeated 10,000 times to form a distribution of median node ages. This process gives conservative estimates, since neither Callitroidea nor Podocarpaceae are that poorly sampled in our dataset (61% and 66% of extant species are present respectively) and Araucariaceae (81% species sampling) is sampled nearly as well as NH clades (84% and 95% species sampling for Pinaceae and Cupressoideae respectively). After resampling, median node ages for NH clades remained significantly older than SH clades (Table S1, Fig. S1*B*)

Southern Hemisphere conifer clades also contain a greater proportion of tropical taxa than NH clades, which could potentially result in differences in divergence times based on broad latitude patterns rather than landmass configuration. However, estimated divergence ages for individual species do not show a strong latitudinal gradient in either hemisphere (Fig. S2). In the Northern Hemisphere, species with extremely recent estimated divergence ages (e.g., 1.0 My or less) occur across a very broad range of latitudes. These species tend to occur in large regions of high conifer diversity, including western North America and southern and southwestern China. In the Southern Hemisphere, species with extremely recent divergence ages are largely absent from all latitudes, although there is a weak positive relationship between high southern latitudes and older species divergence age ($R^2 = 0.11$), which primarily reflects deep divergence times in a subset of extant temperate species of Podocarpaceae.

To test whether differences between Northern and Southern Hemisphere clades resulted from a bias in our divergence time estimates, we also examined raw molecular branch lengths calculated using RAxML in NH and SH focal clades. As discussed in the main text, these results are consistent with our estimated divergence times; median molecular branch lengths are smaller in NH clades than SH clades (Table S2). In particular, NH clades have relatively few long branches and an abundance of extremely short branches compared to SH clades (Fig. S3*A,B*; focal clades significantly different at $p<0.01$ using Mann-Whitney U-test). These differences do not appear to result from biased genetic sampling; NH clades consistently have a greater proportion of short branch lengths when calculated using *rbc*L sequences (Fig. S3*C*) and *mat*K sequences alone (Fig. S3*D*). In both cases, branch length distributions between the focal clades are significantly different at $p<0.01$ using Mann-Whitney U-test).

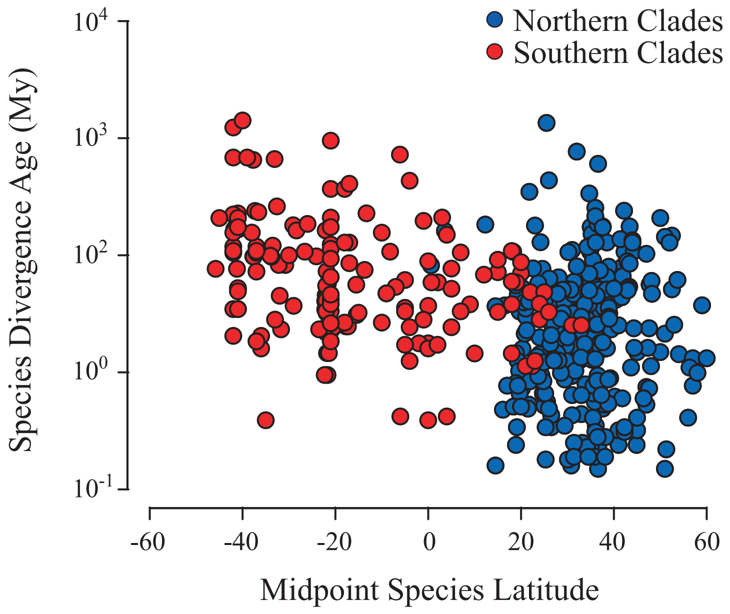

Fig. S2. Relationship between latitude and estimated divergence age (in million of years; My) for individual living conifer species. Species latitudes were determined based on the midpoint of present day geographical range (primarily found in refs. 1-4).

Clade	**Median Molecular Branch Lengths**	
	Observed	50% species resampling
Araucariaceae (SH)	9.1×10^{-4}	-
Podocarpaceae (SH)	1.2×10^{-3}	-
Callitroidea (SH)	3.4×10^{-3}	-
Cupressoidea (NH)	4.3×10^{-4}	4.5×10^{-4}- (7.8×10^{-4}) -1.1×10^{-3}
Pinaceae (NH)	4.0×10^{-4}	4.2×10^{-4}- (5.0×10^{-4}) - 6.1×10^{-4}

Table S2. Median branch lengths for major Southern (SH) and Northern Hemisphere (NH) clades. Branch lengths are given in substitutions per site. Resampled values in parentheses represent the median of 10,000 median branch lengths calculated from a resampling routine where NH clades were reduced to 50% species sampling (see discussion in Supplementary Materials). Values outside of the parentheses give the lower and upper boundaries of the 95% confidence intervals for this distribution.

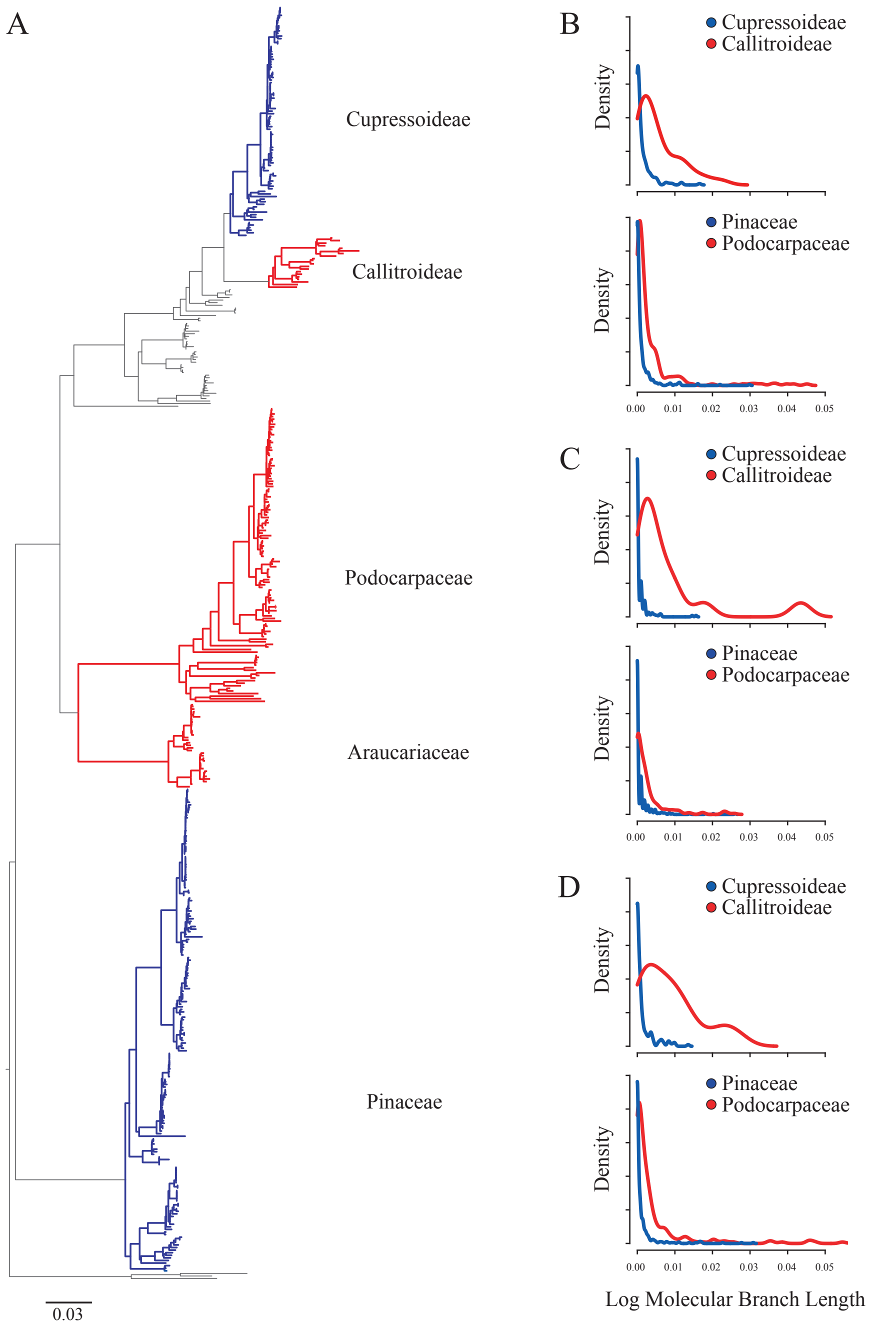

Fig. S3. (*A*) Molecular phylogeny based *rbc*L, *mat*K, 18S and *PHYP* sequences with branch lengths representing raw molecular substitutions per site. Focal clades are labeled and indicated in red (Southern Hemisphere) and blue (Northern Hemisphere) (*B*) Comparison of molecular branch *length* distributions in focal clades based on *rbc*L, *mat*K, 18S and *PHYP*. Lines represent density functions calculated from histograms of branch lengths, which were scaled for comparison. Density values are arbitrary and are not shown on the axes (*C*) Comparison of molecular branch length distributions based on an analysis of *rbc*L sequences only. (*D*) Comparison of molecular branch length distributions based on an analysis *mat*K sequences only.

Diversity Patterns Through Time

We constructed lineage-through-time (LTT) plots for each of the major clades as a way to visualize the timing of speciation events. In addition, to better understand the dynamics of these originations we also assessed the fit of various lineage-specific diversification models. We used recently developed coalescent-based methods that work back from the present to the root of a tree to approximate the likelihood of observing the distribution of internode distances under various diversification scenarios ("backwards" approach; see 7). The coalescent-based approach can readily accommodates incomplete species sampling and is known to outperform “time-forward” methods in both its robustness and its ability to accommodate time-varying rates (7).

We assessed the fit of five diversification scenarios (Table S3). The first corresponds to a hypothesis that diversity is saturated, and is maintained by a turnover process such that an extinction event is immediately followed by a speciation event (Time-constant turnover model). The second model is a generalization of the first, in that the turnover rate decays through time (Time-varying turnover model). The remaining three scenarios assume that diversity is expanding by independent speciation and extinction events that vary in fundamentally different ways. In one scenario, extinction is assumed to be zero, and speciation is allowed to vary (Yule with time-varying speciation). In the remaining two scenarios, the extinction rate is constant, and speciation rates are allowed to vary through time (Birth-Death with time-varying speciation), or speciation rate is assumed to be constant and extinction rate is allowed to vary (Birth-Death with time-varying extinction).

	Saturated Diversity		**Expanding Diversity**		
Clade	**Time-constant Turnover**	**Time-varying Turnover**	**Yule Time-varying Speciation**	**BD Time-varying Speciation**	**BD Time-varying Extinction**
Araucariaceae	0.336 (522)	**0.548 (393)**	0.091 (85)	<0.01 (0)	0.024 (0)
Podocarpaceae	0.021 (0)	**0.979 (1000)**	<0.01 (0)	<0.01 (0)	<0.01 (0)
Callitroideae	0.097 (20)	**0.435 (889)**	0.321 (91)	0.083 (0)	0.063 (0)
Cupressoideae	0.018 (0)	**0.944 (997)**	0.011 (1)	<0.01 (1)	<0.024 (1)
Pinaceae	0.131 (0)	**0.869 (1000)**	<0.01 (0)	<0.01 (0)	<0.01 (0)

Table S3. Average AIC weights across a set of 1000 trees for different diversification models in each of the major conifer clades under study. The numbers in parentheses are the frequencies that each model had the highest AIC weight. Time-varying turnover models were best fit in most clades, with a very slight decrease in turnover rate over time. BD refers to birth-death models with varying speciation and extinction parameters.

A maximum-likelihood based approach was used to obtain parameter estimates and assess the model fit across 1000 trees randomly chosen from the posterior distribution of dated trees. Initial exploratory analyses revealed that the likelihood function was “noisy”, often converging to several different local maximum rather than consistent and potentially global one. To avoid this situation, we implemented an initial “coarse” grid search prior to the full likelihood search to find the set of starting conditions that ensured finding the global maximum (i.e., the highest negative log-likelihood). The AIC weight (w_i), which represents the relative likelihood that model *i* is the best model given a set of models (8), was calculated and averaged for all the models across the 1000 trees. The model with the highest average AIC weight was considered the model with highest probability. All analyses were carried out using scripts written for R (R Development Core Team, 2011).

Time-calibrated Conifer Phylogeny

Fig. S4. A detailed version of the dated phylogenetic tree used in the primary text is given on the following pages, where it has been broken into separate panels showing Cupressaceae and Taxaceae (A), Podocarpaceae and Araucariaceae (B), and Pinaceae (C) respectively. Calibration points are labeled on the tree numerically, and are described in more detail in the following sections. Dashed lines indicate the Paleozoic-Mesozoic boundary (251 My), the Cretaceous-Paleogene boundary (65 My), and the Paleogene-Neogene boundary (23 My; dates from 5). Bars at each node represent 95% confidence intervals for the distribution of estimated divergence times, and the median value of this distribution is illustrated as the divergence time. Blue bars indicate age distributions for nodes whose extant descendant members have a Northern Hemisphere distribution, while red bars indicate nodes where all extant descendant taxa have a Southern Hemisphere or tropical distribution. Gray bars are associated with nodes that have both northern and southern descendant taxa.

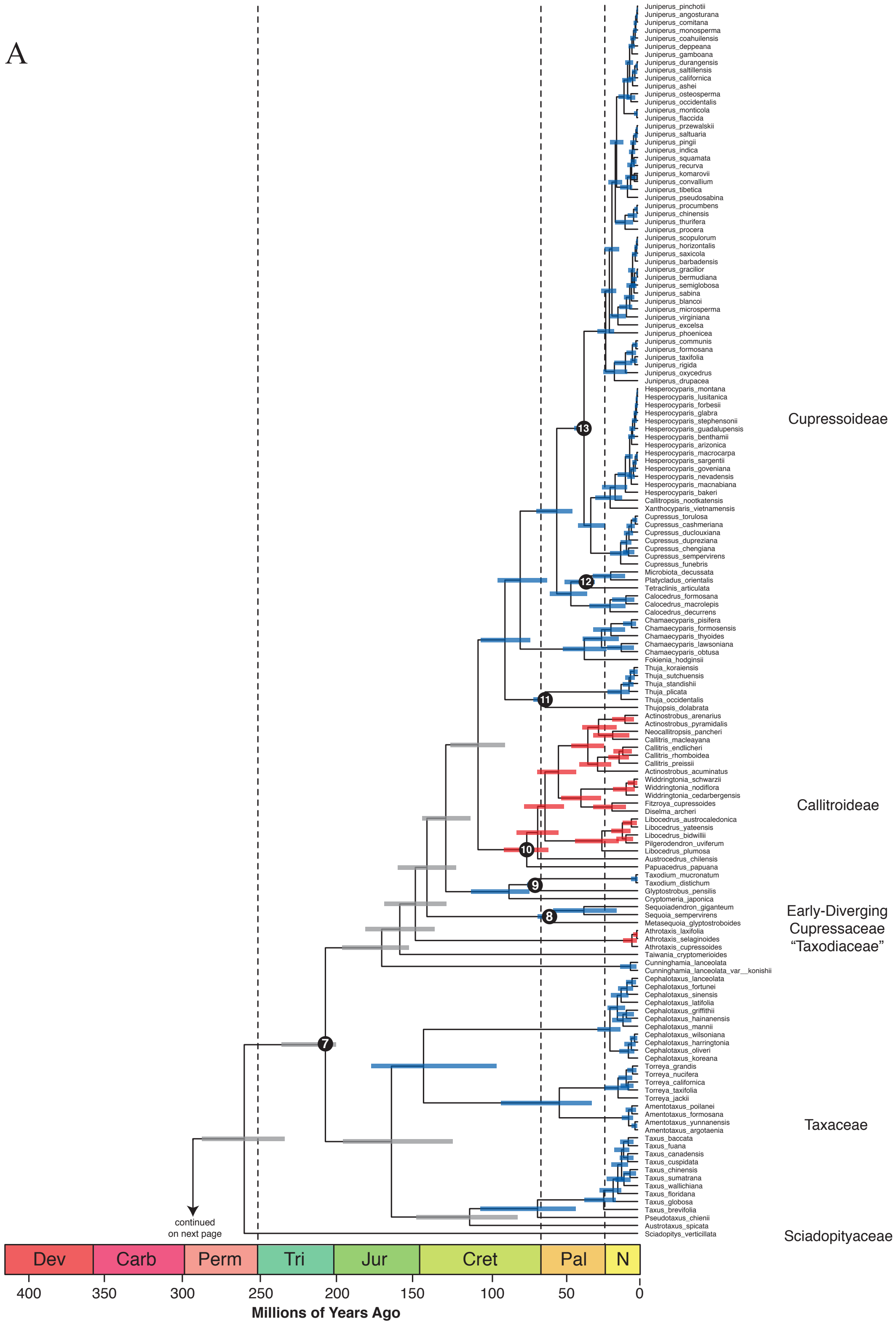
A
Juniperus_pinchotii
Juniperus_angosturana
Juniperus_comitana
Juniperus_monosperma
Juniperus_coahuilensis
Juniperus_deppeana
Juniperus_gamboana
Juniperus_durangensis
Juniperus_saltillensis
Juniperus_californica
Juniperus_ashei
Juniperus_osteosperma
Juniperus_occidentalis
Juniperus_monticola
Juniperus_flaccida
Juniperus_przewalskii
Juniperus_saltuaria
Juniperus_pingii
Juniperus_indica
Juniperus_squamata
Juniperus_recurva
Juniperus_komarovii
Juniperus_convallium
Juniperus_tibetica
Juniperus_pseudosabina
Juniperus_procumbens
Juniperus_chinensis
Juniperus_thurifera
Juniperus_procera
Juniperus_scopulorum
Juniperus_horizontalis
Juniperus_saxicola
Juniperus_barbadensis
Juniperus_gracilior
Juniperus_bermudiana
Juniperus_semiglobosa
Juniperus_sabina
Juniperus_blancoi
Juniperus_microsperma
Juniperus_virginiana
Juniperus_excelsa
Juniperus_phoenicea
Juniperus_communis
Juniperus_formosana
Juniperus_taxifolia
Juniperus_rigida
Juniperus_oxycedrus
Juniperus_drupacea
Hesperocyparis_montana
Hesperocyparis_lusitanica
Hesperocyparis_forbesii
Hesperocyparis_glabra
Hesperocyparis_stephensonii
Hesperocyparis_guadalupensis
Hesperocyparis_benthamii
Hesperocyparis_arizonica
Hesperocyparis_macrocarpa
Hesperocyparis_sargentii
Hesperocyparis_goveniana
Hesperocyparis_nevadensis
Hesperocyparis_macnabiana
Hesperocyparis_bakeri
Callitropsis_nootkatensis
Xanthocyparis_vietnamensis
Cupressus_torulosa
Cupressus_cashmeriana
Cupressus_duclouxiana
Cupressus_dupreziana
Cupressus_chengiana
Cupressus_sempervirens
Cupressus_funebris
Microbiota_decussata
Platycladus_orientalis
Tetraclinis_articulata
Calocedrus_formosana
Calocedrus_macrolepis
Calocedrus_decurrens
Chamaecyparis_pisifera
Chamaecyparis_formosensis
Chamaecyparis_thyoides
Chamaecyparis_lawsoniana
Chamaecyparis_obtusa
Fokienia_hodginsii
Thuja_koraiensis
Thuja_sutchuensis
Thuja_standishii
Thuja_plicata
Thuja_occidentalis
Thujopsis_dolabrata
Actinostrobus_arenarius
Actinostrobus_pyramidalis
Neocallitropsis_pancheri
Callitris_macleayana
Callitris_endlicheri
Callitris_rhomboidea
Callitris_preissii
Actinostrobus_acuminatus
Widdringtonia_schwarzii
Widdringtonia_nodiflora
Widdringtonia_cedarbergensis
Fitzroya_cupressoides
Diselma_archeri
Libocedrus_austrocaledonica
Libocedrus_yateensis
Libocedrus_bidwillii
Pilgerodendron_uviferum
Libocedrus_plumosa
Austrocedrus_chilensis
Papuacedrus_papuana
Taxodium_mucronatum
Taxodium_distichum
Glyptostrobus_pensilis
Cryptomeria_japonica
Sequoiadendron_giganteum
Sequoia_sempervirens
Metasequoia_glyptostroboides
Athrotaxis_laxifolia
Athrotaxis_selaginoides
Athrotaxis_cupressoides
Taiwania_cryptomerioides
Cunninghamia_lanceolata
Cunninghamia_lanceolata_var__konishii
Cephalotaxus_lanceolata
Cephalotaxus_fortunei
Cephalotaxus_sinensis
Cephalotaxus_latifolia
Cephalotaxus_griffithii
Cephalotaxus_hainanensis
Cephalotaxus_mannii
Cephalotaxus_wilsoniana
Cephalotaxus_harringtonia
Cephalotaxus_oliveri
Cephalotaxus_koreana
Torreya_grandis
Torreya_nucifera
Torreya_californica
Torreya_taxifolia
Torreya_jackii
Amentotaxus_poilanei
Amentotaxus_formosana
Amentotaxus_yunnanensis
Amentotaxus_argotaenia
Taxus_baccata
Taxus_fuana
Taxus_canadensis
Taxus_cuspidata
Taxus_chinensis
Taxus_sumatrana
Taxus_wallichiana
Taxus_floridana
Taxus_globosa
Taxus_brevifolia
Pseudotaxus_chienii
Austrotaxus_spicata
Sciadopitys_verticillata
13
12
11
10
9
8
7
Cupressoideae
Callitroideae
Early-Diverging
Cupressaceae
“Taxodiaceae”
Taxaceae
Sciadopityaceae
continued
on next page
Dev
Carb
Perm
Tri
Jur
Cret
Pal
N
400
350
300
250
200
150
100
50
0
Millions of Years Ago

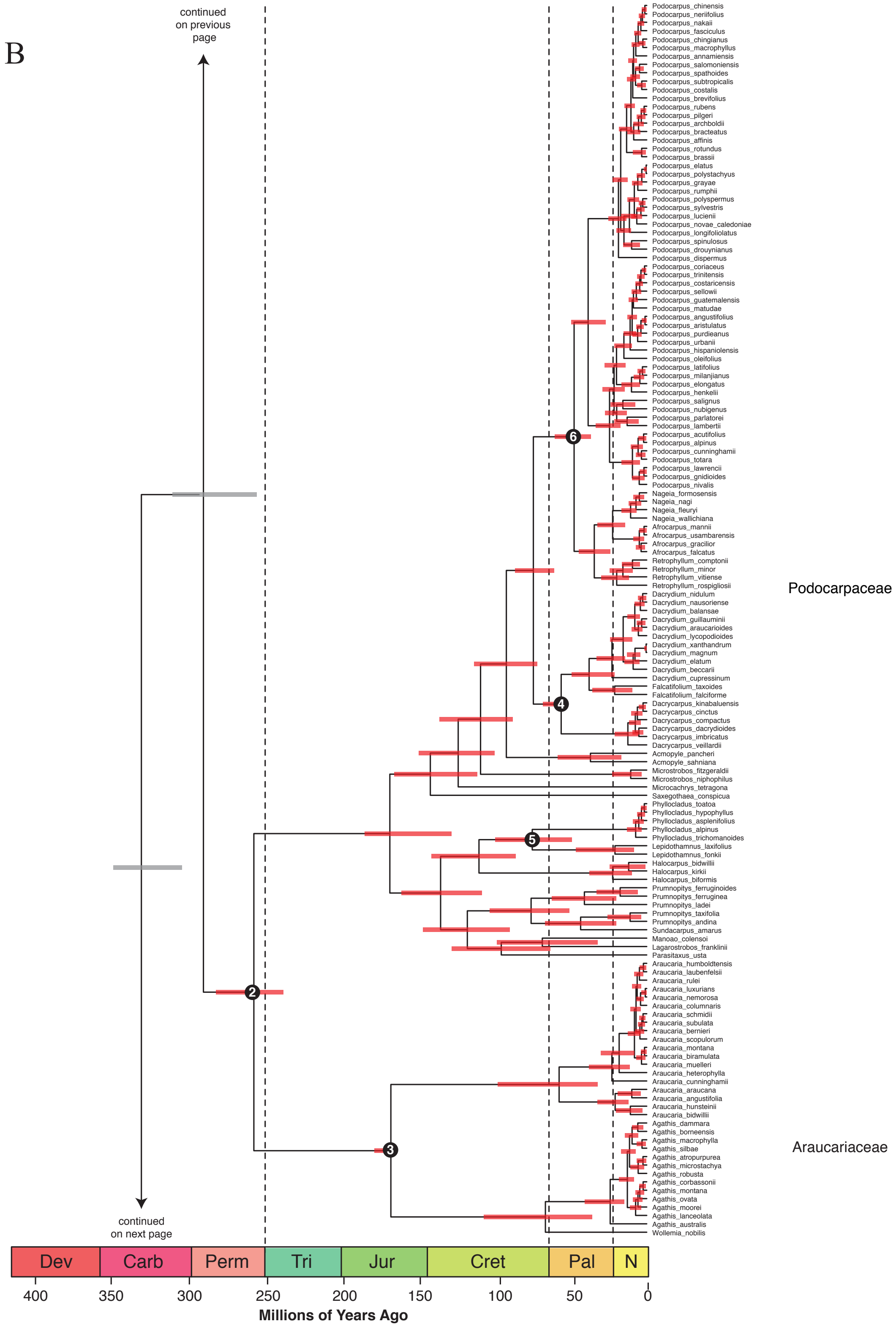
B
continued
on previous
page
continued
on next page
Podocarpus_chinensis
Podocarpus_neriifolius
Podocarpus_nakaii
Podocarpus_fasciculus
Podocarpus_chingianus
Podocarpus_macrophyllus
Podocarpus_annamiensis
Podocarpus_salomoniensis
Podocarpus_spathoides
Podocarpus_subtropicalis
Podocarpus_costalis
Podocarpus_brevifolius
Podocarpus_rubens
Podocarpus_pilgeri
Podocarpus_archboldii
Podocarpus_bracteatus
Podocarpus_affinis
Podocarpus_rotundus
Podocarpus_brassii
Podocarpus_elatus
Podocarpus_polystachyus
Podocarpus_grayae
Podocarpus_rumphii
Podocarpus_polyspermus
Podocarpus_sylvestris
Podocarpus_lucienii
Podocarpus_novae_caledoniae
Podocarpus_longifoliolatus
Podocarpus_spinulosus
Podocarpus_drouynianus
Podocarpus_dispermus
Podocarpus_coriaceus
Podocarpus_trinitensis
Podocarpus_costaricensis
Podocarpus_sellowii
Podocarpus_guatemalensis
Podocarpus_matudae
Podocarpus_angustifolius
Podocarpus_aristulatus
Podocarpus_purdieanus
Podocarpus_urbanii
Podocarpus_hispaniolensis
Podocarpus_oleifolius
Podocarpus_latifolius
Podocarpus_milanjianus
Podocarpus_elongatus
Podocarpus_henkelii
Podocarpus_salignus
Podocarpus_nubigenus
Podocarpus_parlatorei
Podocarpus_lambertii
Podocarpus_acutifolius
Podocarpus_alpinus
Podocarpus_cunninghamii
Podocarpus_totara
Podocarpus_lawrencii
Podocarpus_gnidioides
Podocarpus_nivalis
Nageia_formosensis
Nageia_nagi
Nageia_fleuryi
Nageia_wallichiana
Afrocarpus_mannii
Afrocarpus_usambarensis
Afrocarpus_gracilior
Afrocarpus_falcatus
Retrophyllum_comptonii
Retrophyllum_minor
Retrophyllum_vitiense
Retrophyllum_rospigliosii
Dacrydium_nidulum
Dacrydium_nausoriense
Dacrydium_balansae
Dacrydium_guillauminii
Dacrydium_araucarioides
Dacrydium_lycopodioides
Dacrydium_xanthandrum
Dacrydium_magnum
Dacrydium_elatum
Dacrydium_beccarii
Dacrydium_cupressinum
Falcatifolium_taxoides
Falcatifolium_falciforme
Dacrycarpus_kinabaluensis
Dacrycarpus_cinctus
Dacrycarpus_compactus
Dacrycarpus_dacrydioides
Dacrycarpus_imbricatus
Dacrycarpus_veillardii
Acmopyle_pancheri
Acmopyle_sahniana
Microstrobos_fitzgeraldii
Microstrobos_niphophilus
Microcachrys_tetragona
Saxegothaea_conspicua
Phyllocladus_toatoa
Phyllocladus_hypophyllus
Phyllocladus_asplenifolius
Phyllocladus_alpinus
Phyllocladus_trichomanoides
Lepidothamnus_laxifolius
Lepidothamnus_fonkii
Halocarpus_bidwillii
Halocarpus_kirkii
Halocarpus_biformis
Prumnopitys_ferruginoides
Prumnopitys_ferruginea
Prumnopitys_ladei
Prumnopitys_taxifolia
Prumnopitys_andina
Sundacarpus_amarus
Manoao_colensoi
Lagarostrobos_franklinii
Parasitaxus_usta
Araucaria_humboldtensis
Araucaria_laubenfelsii
Araucaria_rulei
Araucaria_luxurians
Araucaria_nemorosa
Araucaria_columnaris
Araucaria_schmidii
Araucaria_subulata
Araucaria_bernieri
Araucaria_scopulorum
Araucaria_montana
Araucaria_biramulata
Araucaria_muelleri
Araucaria_heterophylla
Araucaria_cunninghamii
Araucaria_araucana
Araucaria_angustifolia
Araucaria_hunsteinii
Araucaria_bidwillii
Agathis_dammara
Agathis_borneensis
Agathis_macrophylla
Agathis_silbae
Agathis_atropurpurea
Agathis_microstachya
Agathis_robusta
Agathis_corbassonii
Agathis_montana
Agathis_ovata
Agathis_moorei
Agathis_lanceolata
Agathis_australis
Wollemia_nobilis
6
4
5
2
3
Podocarpaceae
Araucariaceae
Dev
Carb
Perm
Tri
Jur
Cret
Pal
N
400
350
300
250
200
150
100
50
0
Millions of Years Ago

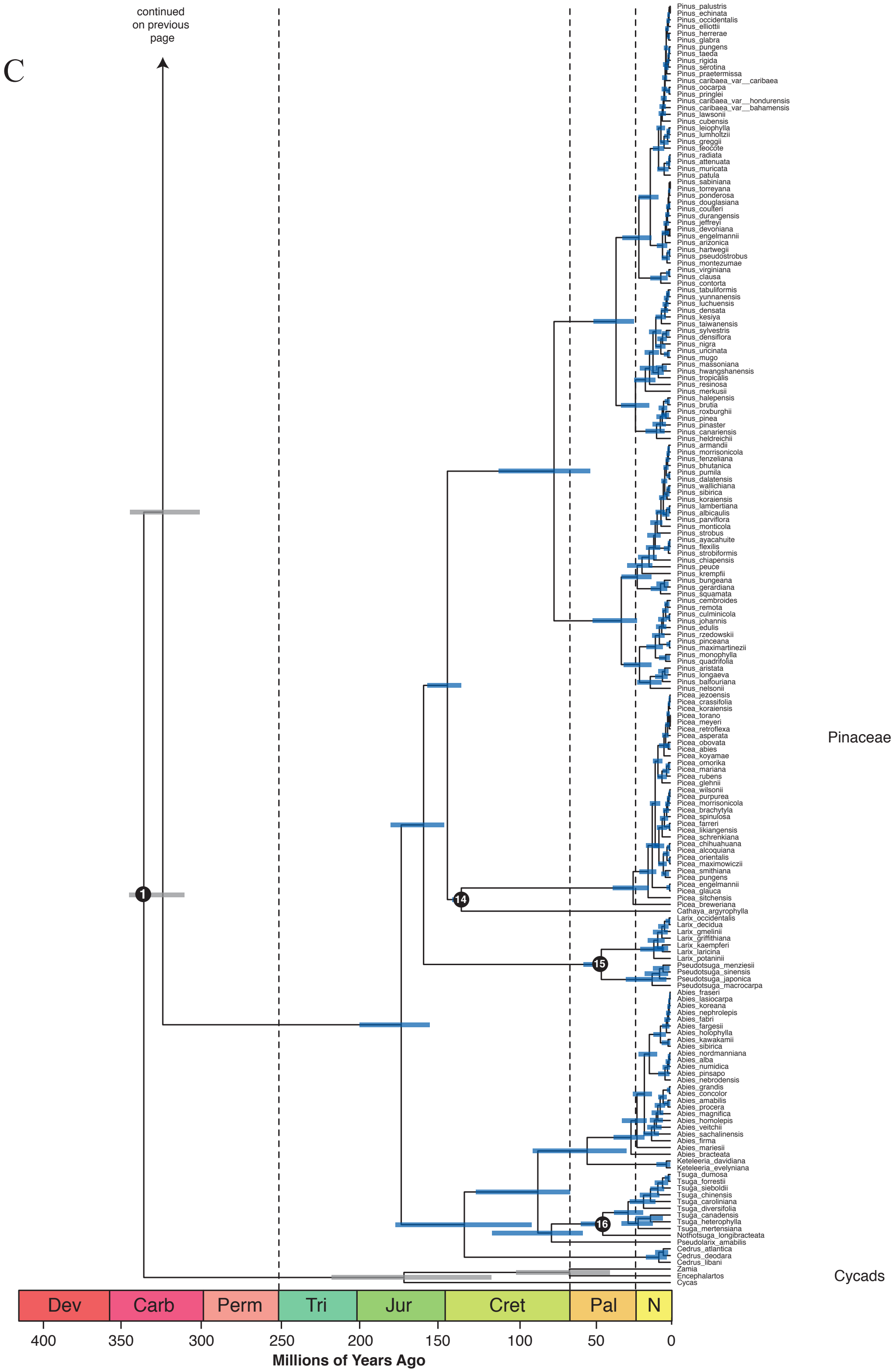C
continued on previous page
1
14
15
16
Pinus_palustris
Pinus_echinata
Pinus_occidentalis
Pinus_elliottii
Pinus_herrerae
Pinus_glabra
Pinus_pungens
Pinus_taeda
Pinus_rigida
Pinus_serotina
Pinus_praetermissa
Pinus_caribaea_var__caribaea
Pinus_oocarpa
Pinus_pringlei
Pinus_caribaea_var__hondurensis
Pinus_caribaea_var__bahamensis
Pinus_lawsonii
Pinus_cubensis
Pinus_leiophylla
Pinus_lumholtzii
Pinus_greggii
Pinus_teocote
Pinus_radiata
Pinus_attenuata
Pinus_muricata
Pinus_patula
Pinus_sabiniana
Pinus_torreyana
Pinus_ponderosa
Pinus_douglasiana
Pinus_coulteri
Pinus_durangensis
Pinus_jeffreyi
Pinus_devoniana
Pinus_engelmannii
Pinus_arizonica
Pinus_hartwegii
Pinus_pseudostrobus
Pinus_montezumae
Pinus_virginiana
Pinus_clausa
Pinus_contorta
Pinus_tabuliformis
Pinus_yunnanensis
Pinus_luchuensis
Pinus_densata
Pinus_kesiya
Pinus_taiwanensis
Pinus_sylvestris
Pinus_densiflora
Pinus_nigra
Pinus_uncinata
Pinus_mugo
Pinus_massoniana
Pinus_hwangshanensis
Pinus_tropicalis
Pinus_resinosa
Pinus_merkusii
Pinus_halepensis
Pinus_brutia
Pinus_roxburghii
Pinus_pinea
Pinus_pinaster
Pinus_canariensis
Pinus_heldreichii
Pinus_armandii
Pinus_morrisonicola
Pinus_fenzeliana
Pinus_bhutanica
Pinus_pumila
Pinus_dalatensis
Pinus_wallichiana
Pinus_sibirica
Pinus_koraiensis
Pinus_lambertiana
Pinus_albicaulis
Pinus_parviflora
Pinus_monticola
Pinus_strobus
Pinus_ayacahuite
Pinus_flexilis
Pinus_strobiformis
Pinus_chiapensis
Pinus_peuce
Pinus_krempfii
Pinus_bungeana
Pinus_gerardiana
Pinus_squamata
Pinus_cembroides
Pinus_remota
Pinus_culminicola
Pinus_johannis
Pinus_edulis
Pinus_rzedowskii
Pinus_pinceana
Pinus_maximartinezii
Pinus_monophylla
Pinus_quadrifolia
Pinus_aristata
Pinus_longaeva
Pinus_balfouriana
Pinus_nelsonii
Picea_jezoensis
Picea_crassifolia
Picea_koraiensis
Picea_torano
Picea_meyeri
Picea_retroflexa
Picea_asperata
Picea_obovata
Picea_abies
Picea_koyamae
Picea_omorika
Picea_mariana
Picea_rubens
Picea_glehnii
Picea_wilsonii
Picea_purpurea
Picea_morrisonicola
Picea_brachytyla
Picea_spinulosa
Picea_farreri
Picea_likiangensis
Picea_schrenkiana
Picea_chihuahuana
Picea_alcoquiana
Picea_orientalis
Picea_maximowiczii
Picea_smithiana
Picea_pungens
Picea_engelmannii
Picea_glauca
Picea_sitchensis
Picea_breweriana
Cathaya_argyrophylla
Larix_occidentalis
Larix_decidua
Larix_gmelinii
Larix_griffithiana
Larix_kaempferi
Larix_laricina
Larix_potaninii
Pseudotsuga_menziesii
Pseudotsuga_sinensis
Pseudotsuga_japonica
Pseudotsuga_macrocarpa
Abies_fraseri
Abies_lasiocarpa
Abies_koreana
Abies_nephrolepis
Abies_fabri
Abies_fargesii
Abies_holophylla
Abies_kawakamii
Abies_sibirica
Abies_nordmanniana
Abies_alba
Abies_numidica
Abies_pinsapo
Abies_nebrodensis
Abies_grandis
Abies_concolor
Abies_amabilis
Abies_procera
Abies_magnifica
Abies_homolepis
Abies_veitchii
Abies_sachalinensis
Abies_firma
Abies_mariesii
Abies_bracteata
Keteleeria_davidiana
Keteleeria_evelyniana
Tsuga_dumosa
Tsuga_forrestii
Tsuga_sieboldii
Tsuga_chinensis
Tsuga_caroliniana
Tsuga_diversifolia
Tsuga_canadensis
Tsuga_heterophylla
Tsuga_mertensiana
Nothotsuga_longibracteata
Pseudolarix_amabilis
Cedrus_atlantica
Cedrus_deodara
Cedrus_libani
Zamia
Encephalartos
Cycas
Pinaceae
Cycads
Dev
Carb
Perm
Tri
Jur
Cret
Pal
N
400
350
300
250
200
150
100
50
0
Millions of Years Ago

Summary of Calibration Points and Priors

The age ranges (in My) shown represent the 95% confidence intervals for the 20 My lognormal prior. Figures given in parentheses are for the 40 My prior. See text below for more detailed information concerning these age ranges, particularly for the divergences (2. Araucariaceae – Podocarpaceae, 6. *Podocarpus – Retrophyllum*, 16. *Tsuga – Nothotsuga*) in which the typical 20 and 40 My prior age distributions were modified.

1. Conifer divergence. Uniform prior: 275-350 My

2. Araucariaceae - Podocarpaceae divergence. Lognormal prior: 176-230 My

3. *Araucaria* – (*Wollemia* + *Agathis*) divergence. Lognormal prior: 165-185 (205) My

4. *Dacrycarpus* – (*Falcatifolium*+*Dacrydium*) divergence. Lognormal prior: 51.9-71.9 (91.9) My

5. *Phyllocladus – Lepidothamnus* divergence. Lognormal prior: 48-68 (88) My

6. *Podocarpus – Retrophyllum* divergence. Lognormal prior: 28-60 (80) My

7. Taxaceae – Cupressaceae divergence. Lognormal prior: 197- 217 (237) My

8. *Metasequoia* – (*Sequoia*+*Sequoiadendron*) divergence. Lognormal prior: 55-75 (95) My

9. *Taxodium – Glyptostrobus* divergence. Lognormal prior: 65-85 (105) My

10. *Papuacedrus* – (other Callitroids) divergence. Lognormal prior: 51.9-71.9 (91.9) My

11. *Thuja – Thujopsis* divergence. Lognormal prior: 58-78 (98) My

12. *Tetraclinis* – (*Platycladus*+*Microbiota*) divergence. Lognormal prior: 28-48 (68) My

13. *Juniperus – Cupressus* sensu lato divergence. Lognormal prior: 33-53 (73) My

14. *Picea- Cathaya* divergence. Lognormal prior: 133-153 (173) My

15. *Larix – Pseudotsuga* divergence. Lognormal prior: 41-61 (81) My

16. *Tsuga – Nothotsuga* divergence. Lognormal prior: 41-90 (100) My

Details and Discussion of Calibration Points and Priors

1. Conifer divergence

Fossils: Upper bound based on megasporophylls that are morphologically similar to extant *Cycas* from the uppermost Lower Permian of China (*Crossozamia* spp. ~275 My; 9). Lower bound based on the appearance of ovules with a fully fused integument similar to that of all living seed plant groups in the Lower Carboniferous (350 My; 10).

Prior: Uniform; 275-350 My

Discussion: Extant cycads are often thought to be related to medullosan seed ferns (11), suggesting that the first appearance of medullosans in the fossil record (*Quaestora*; Late Mississippian ~320 My; 12) could be used as a minimum age for the cycad-conifer split. However, recent cladistic analyses have not generally supported a close relationship, suggesting instead that lyginopterid and medullosan seed ferns form an early grade of seed plants no more closely related to living cycads than other extant groups (13-15). In this context, the first appearance of megasporophylls that are morphologically similar to those of extant *Cycas* (Early Permian ~275 My; 9) are here used as the minimum age for the conifer – cycad divergence. The first appearance of conifers or conifer-like plants in the Pennsylvanian is not used as the minimum age because pollination and fertilization in these plants is unlike modern conifers and is more similar to primitive seed plant groups (for example, they were most likely zooidogamous). This may suggest that these plants are not closely related to modern conifers (see 13), even though Paleozoic conifers have been linked with living conifers based on other shared aspects of their vegetative and reproductive morphology as well as in more recent phylogenetic analyses (14,15). The first appearance of derived conifer or conifer-like traits could potentially be used as the minimum age for the divergence of living conifers from other groups of extant seed plants, but they fall within the uniform prior employed here. Saccate pollen grains similar those produced by younger Paleozoic conifer and conifer-like macrofossils (*Florinites*, *Potoniesporites*) enter the fossil record in the Serpukovian (~326 My; 16). Diverse saccate pollen, including bisaccate forms characteristic of extant conifers but also many other groups of extinct gymnosperms, are known from the early Bashkirian (~317 My; 17) and may suggest early conifers were present for some time before their recognition as macrofossils.

In light of the uncertainty regarding the first appearance of early conifers and their exact phylogenetic placement, we extend the maximum age of the cycad-conifer divergence to the earliest evidence of seed plants with a fused integument, a trait shared by all living groups but that is not present in the earliest seed plants. This feature appears as early as the Tournasian in the lowermost Carboniferous (~350 My; see 10), and was also used by Crisp and Cook (18) to set the lower boundary of the divergence of extant seed plant groups. We use this date so that we do not potentially bias our analyses toward younger dates for this divergence, but there is no fossil evidence from either palynology or reproductive morphology that suggests early members belonging to the five living seed plant groups were present before the Serpukovian (~326 My). Early ovules with a fully fused integument also retain morphological features suggesting a more primitive pollination biology that is not shared with any living gymnosperm, including tetrahedral division of the megaspore mother cell, an elaborate nucellar pollen chamber for receiving pollen, and the hydrasperman-type pollination biology characteristic of primitive seed plants (see 15).

2. Araucariaceae – Podocarpaceae divergence

Fossils: Presence of *Araucariacites* pollen grains in conjunction with the earliest macrofossils putatively assigned to *Araucariaceae* (*Araucarites rudicula*; Late Carnian, ~230 My; 19). Unambiguous evidence of Araucariaceae by the Aalenian (172-176 My) based on *Araucaria*-like ovulate cones and scales (*Araucarites phillipsii*) as well as pollen cones (attached to *Brachyphyllum mammilare* foliage) containing pollen comparable to *Araucariacites* and living Araucariaceae (20).

Prior: Lognormal; 172-230 My (95% confidence intervals)

Discussion: Several Middle Triassic fossils have been considered to represent early Podocarpaceae, and have been used to date the split between this family and the Araucariaceae (see excluded fossils below). However, fossils with ovulate cones that are comparable to those of living Podocarpaceae do not enter the record until the Middle Jurassic (20) and the earliest appearance of unambiguous Podocarpaceae is not until the Early Cretaceous (e.g., 21), well after the earliest appearance of unambiguous Araucariaceae. Therefore, we use the more definitive early record of the Araucariaceae to constrain the divergence of these two families.

Pollen grains similar to those of modern Araucariaceae (*Araucariacites*) are first described from the Early Triassic (22), and are also known from the Middle-Late Triassic of Patagonia (23) and the Late Triassic of Europe (24). Although *Araucariacites* and similar palynomorphs therefore have a substantial Triassic record, so far they have not been found associated with reproductive structures until the Middle Jurassic. In general, *Araucariacites* (and the potential araucarian grain *Inaperturopollenites*, which is also applied to pollen grains of Cupressaceae *sensu lato*) are similar to the pollen of living Araucariaceae in that they are relatively large, non-saccate, and have a granular surface ornamentation. However, these are not sufficiently definitive characters to securely infer the presence of either stem or crown group Araucariaceae.

The earliest potential macrofossils of Araucariaceae consists of ovulate cones and isolated scales preserved as compression or impression fossils in several Late Triassic macrofloras (19*,* 25, 26). However, due to their poor preservation, it is difficult to assign them unambiguously to the Araucariaceae. The isolated scales are usually broadly triangular and bear a single large ovule or seed, although they lack evidence of an ovule scale, or ligule, which is characteristic of the extant genus *Araucaria* (although not the extant genera *Wollemia* or *Agathis*). The earliest dated occurrence of these of triangular, non-ligulate scales (*Araucarites rudicula*; 19) is used to define the lower 95% confidence interval on our lognormal prior age distribution in order to allow for the possibility that these specimens are related to extant Araucariaceae. These fossils have been dated to the late Carnian– middle Norian (~230-213 My) by palynology and detrital zircons (27, 28). However, we do not consider scales of this kind to be unambiguous evidence of the family because they differ in their overall morphology from unambiguous Middle Jurassic Araucariaceae (a ligule is lacking and they have relatively small ovules with a highly constricted scale base), their anatomy is not preserved, and they lack co-occurring foliage or palynomorphs that would help support placement in the family.

We set minimum age for the Podocarpaceae – Araucariaceae split by the first appearance of fossils we consider to be unambiguous evidence of stem or crown Araucariaceae (*Araucarites phillipsii* cone and associated *Brachyphyllum mammilare* foliage with attached pollen cones) from the Aalenian (172-176 My). Harris (20) considered these fossils to belong to the same plant based on their common co-occurrence and similar cuticular morphology, and both could independently be assigned to the Araucariaceae based on their morphology. Pollen cones attached to *Brachyphyllum mammilare* foliage produced relatively large, non-saccate pollen comparable to modern *Araucaria* (29) and the foliage also contains oval sclereids similar to those found in extant *Araucaria cunninghamiii*. *Araucarites phillipsii* seed cones consist of broad cone scales in which the ovule scale appears to be fused to the bract for most of its length but is separated at the tip. The material is not permineralized but the ovule or seed is interpreted as being covered by cone scale tissue as in extant Araucariaceae. Due to the preservation, it is not possible to definitely assign this species to a living section of *Araucaria*, but it has been linked to Section *Eutacta* (20; 30). Using the minimum age of 172 My, in this instance we use a lognormal prior of 58 My to accommodate the possibility that the late Carnian – middle Norian fossils are related to extant Araucariaceae (see above).

The *Brachphyllum – Araucarites phillipsii* plant may represent definitive evidence of the divergence of *Araucaria* based on the wingless seed (*Agathis* and *Wollemia* seeds are winged) and the presence of a free ligule tip (*Agathis* and *Wollemia* lack the ligule tip and their ovule scale is completely fused to the bract). However, since these fossils are not anatomically preserved and because the exact sequence of character changes occurring in ovulate scale evolution in early *Araucariaceae* are not entirely clear (see also below), we do not use it to date the *Araucaria* – (*Agathis*+*Wollemia*) divergence.

3. *Araucaria* – (*Wollemia* + *Agathis*) divergence

Fossils: *Araucaria sphaerocarpa* (31) from the Inferior Oolite at Bruton Station, Somerset, UK. At this locality, the Inferior Oolite has yielded ammonites suggesting a Middle Bathonian age, although they do not appear to have been recovered from the limestone where this species was found. Deposition of the Upper Inferior Oolite in southern England ends at the very beginning of the Bathonian (32), so it is likely that the deposits yielding *A. sphaerocarpa* span the Bajocian-Bathonian boundary (33). We therefore set the minimum age at the end of the Bathonian (165 My).

Prior: Lognormal; 165-185 (205) My (95% confidence intervals)

Discussion: *Araucaria sphaerocarpa* is known from a large cone embedded in marine limestone. It is assigned to Araucariaceae based on its large size, its expanded cone axis, cone scales with single ovules, and the presence of branched zig-zag sclereids in the seed sclerotesta. Assignment to *Araucaria* is based on the wingless seed and a well-developed ligule on the cone scale. Assignment to Section *Bunya* of extant *Araucaria* (containing the living species *A. bidwillii*) is based on the woody winged bract, the complex vascularization of the ovule scale (especially the complex vascular "plexus" at the chalazal end of the ovule), and the separate vascular strands that supply the ovule scale and the bract (all other living sections of *Aracuaria* have a single vascular trace for both). Very similar characteristics of the ovulate scale are found in the slightly younger and better preserved *Araucaria mirabilis* cones from Patagonia (34), although the errors associated with dating the Patagonian localities (157 +/- 10 My) suggest these fossils could be more or less contemporaneous with *A. sphaerocarpa* (35). The placement of both *A. sphaerocarpa* and *A. mirabilis* in Section *Bunya* is strongly suggested by their ovulate scale morphology, although molecular evidence does not place living Section *Bunya* as sister to other *Araucaria* or to Araucariaceae, and the foliage and seedlings associated with these early Araucariaceae (e.g., *A. mirabilis*) are not similar to those of modern Section *Bunya* (30). The fossils could therefore be interpreted in two ways: either Section *Bunya* has been present since the Middle Jurassic while evidence of its sister taxon (Section *Intermedia*; *Araucaria hunsteinii*) only enters fossil record much later in the Late Cretaceous (30), or that extant Section *Bunya* is a younger taxon that preserves the pleisiomorphic ovulate features of *Araucaria* that have been lost independently in the other living sections.

In an earlier version of this study, we implemented these interpretations and explored their effects on our results. In one analysis, ages within the Araucariaceae were not constrained (referred to as No *Araucaria*, No *Bunya* analysis) while in a second, *A. sphaerocarpa* was used to date the divergence between extant *Araucaria* and its sister clade consisting of extant *Agathis* and *Wollemia* (the *Araucaria*, No *Bunya* analysis). Finally, *A. sphaerocarpa* was used to set the minimum age for the divergence between extant Section *Bunya* (which includes the living species *A. bidwillii*) and its sister taxon, Section *Intermedia* (which includes the living species *A. hunsteinii*). These different calibration schemes had little overall impact on estimated divergences times beyond the small clades directly affected (Table S4). Even within Araucariaceae, dating a crown group divergence (the Section *Intermedia* and Section *Bunya* split) to the Middle Jurassic did not greatly alter the median node age for the clade, as the other divergence time estimates within it remained relatively unchanged. In this study, we chose to use *A. sphaerocarpa* to date the first appearance of the *Araucaria* genus.

Clade	Median Node Age in *Araucaria* Calibration Schemes		
	No *Araucaria* No *Bunya*	*Araucaria* No *Bunya*	*Bunya*
Araucariaceae (SH)	4.58	5.04	5.05
Podocarpaceae (SH)	7.04	7.35	7.85
Callitroidea (SH)	14.62	14.97	15.63
Cupressoidea (NH)	3.04 (4.34)	3.31 (4.92)	3.43 (5.13)
Pinaceae (NH)	2.69 (4.17)	2.95 (4.40)	3.04 (4.73)

Table S4. Median node ages (in millions of years; My) for major Southern Hemisphere (SH) and Northern Hemisphere (NH) clades using different calibration schemes based on the interpretation of the Araucariaceae fossil record. Ages are derived from an earlier version of the analyses whose results are not otherwise presented in this study. Ages in parentheses represent the median value of 10,000 median node ages derived from a resampling routine where NH clades were reduced to 50% species sampling.

4. *Dacrycarpus* – (*Falcatifolium*+*Dacrydium*) divergence

Fossils: *Dacrycarpus puertae* from the Laguna del Hunco Flora of Argentina (36), radiometrically dated to the Early Eocene (51.9 My).

Prior: Lognormal; 51.9-71.9 (91.9) My (95% confidence intervals)

Discussion: This species is very similar in reproductive and vegetative morphology to living *Dacrycarpus*, especially *D. imbricatus*. It includes foliage with attached pollen cones and ovulate structures, which also exhibit the warty receptacle characteristic of the genus. The fossil material differs from extant *D. imbricatus* only in a few continuous variables, such as the size of bracts subtending the cones, but was assigned to a separate species because not all aspects of the whole plant are known. We therefore use this fossil conservatively to date the appearance of crown *Dacrycarpus*, rather than the divergence between *D. imbricatus* and its sister species (a clade of *D. kinabaluensis* and *D. cinctus*).

5. *Phyllocladus* – *Lepidothamnus* divergence

Fossils: Phylloclades are described from the mid-Late Eocene (~37 My; 37), as well as from the Early Eocene (48-55 My) of Tasmania (mentioned in Hill and Brodbribb (38).

Prior: Lognormal; 48-68 (88) My (95% confidence intervals)

Discussion: *Phyllocladus* has extremely distinctive, flattened photosynthetic shoots that are unlike any other living conifer. Thus there is little doubt about the assignment of fossils with similar foliage to the *Phyllocladus* lineage, and they are readily identifiable without detailed cuticular or anatomical analysis. However, we treat these fossils as stem taxa and do not attempt to place them within the crown because other features of these plants are unknown and their relationship to particular extant species of *Phyllocladus* is unclear.

6. *Podocarpus – Retrophyllum* divergence

Fossils: *Retrophyllum australe* from the West Dale Flora of southwestern Australia (39), which is dated to the Middle Eocene to Oligocene (28-48 My).

Prior: Lognormal; 28-60 (80) My (95% confidence intervals)

Discussion: *Retrophyllum* has distinctive heterofacially flattened foliage, where leaves on opposite sides of the branch axis twist in opposite directions; therefore the upper surface of the leafy shoot is formed by the abaxial side of one leaf rank and the adaxial side of the other. The same kind of heterofacially flattened foliage also occurs in *Nageia* and *Afrocarpus* (which belong to the clade containing *Retrophyllum*), but these taxa lack the prominent midvein seen in *Retrophyllum*. *Retrophyllum australe* is assigned to extant *Retrophyllum* based on the presence of a midvein, its heterofacially flattened foliage, and its cuticular morphology, which consists of straight epidermal cells, stomata on both sides of the leaf, and prominent Florin rings. However, we do not use *R. australe* as unambiguous evidence of *Retrophyllum* due to uncertainty in placing these fossils in the crown group of the genus. Since *Podocarpus* also has a prominent midvein, this feature most likely represents the pleisiomorphic condition in the *Retrophyllum*/*Afrocarpus*/*Nageia* clade. However, we use *R. australe* to indicate the minimum age for the appearance of the extant clade characterized by heterofacially flattened foliage (the *Retrophyllum*+*Afrocarpus*+*Nageia* clade). Given the very poor constraint on the age of this fossil we used wider priors than in most other calibrations (32 and 52 My respectively).

7. Taxaceae – Cupressaceae divergence

Fossils: *Palaeotaxus rediviva* from the Upper coal bed of the Skromberga Colliery in Scania, Sweden (40). This deposit has been dated to the Lowermost Jurassic (Hettangian, 201-197 My).

Prior: Lognormal; 197- 217 (237) My (95% confidence intervals)

Discussion: *Palaeotaxus rediviva* is similar to modern Taxaceae in having an axillary short shoot bearing sterile scales that terminates in a single ovule. According to Florin (40) the ovule is also surrounded by an aril, although this is difficult to see in the figured specimens (see 41). Regardless of the presence or absence of the aril, the position and form of the ovule strongly suggest this fossil belongs to the lineage that includes extant Taxaceae, because no other conifer family produces reduced axillary ovulate cones with single terminal ovules. Sterile scales on *P. rediviva* seed cones are helically arranged, similar to extant *Austrotaxus* and *Taxus* (whereas *Amentotaxus* and *Torreya* have decussate scales) and the leafy shoots of *Palaeotaxus* are also broadly similar to those of some modern Taxaceae in having spirally arranged, bifacially flattened leaves with a single midvein that form distichous rows on the shoot. Florin hesitated to include *Palaeotaxus* within the modern family due to its unusual cuticular morphology, particularly the wavy epidermal cell walls that are unlike any living genus. We therefore treat *Palaeotaxus* as a minimum age estimate for the divergence between Taxaceae *sensu lato* (including *Cephalotaxus*) and Cupressaceae *sensu lato*.

Depending on the topology of the tree, *Palaeotaxus* could be used to date the Cephalotaxaceae – Taxaceae divergence, since its reduced ovulate cones would appear to place it securely along the Taxaceae lineage. However, this interpretation requires that the sister group relationship of Cephalotaxaceae and Taxaceae is secure and some molecular data (including ours), suggest that *Cephalotaxus* is nested within genera traditionally included in Taxaceae. Specifically, it is resolved as sister to a *Torreya – Amentotaxus* clade in some analyses whereas in others it is resolved as sister to the *Taxus* clade (42). In both these cases, the cone morphology of *Cephalotaxus* is interpreted either a derived elaboration of an ancestrally reduced axis or a retention of the pleisiomorphic condition which requires two separate clades (the *Taxus* clade and the *Torreya* clade) have independently reduced the ovulate cone. Given the uncertainty in the interpretation of the aril in *Palaeotaxus*, combined with the uncertainty of the phylogenetic relationships between *Cephalotaxus* and other Taxaceae, it is not prudent to use *Palaeotaxus* to date the *Cephalotaxus*/*Taxaceae* split. However, its extremely simple ovulate cone, consisting of a single ovule, does at least provide a minimum age for the divergence between Taxaceae broadly considered from the Cupressaceae *sensu lato* clade.

8. *Metasequoia* – (*Sequoia*+*Sequoiadendron*) divergence

Fossils: *Metasequoia occidentalis* from the Wuyun Formation in China (43), dated to the Paleocene (44)

Prior: Lognormal; 55-75 (95) My (95% confidence intervals)

Discussion: *Metasequoia occidentalis* is a whole plant reconstruction that is very similar to modern *Metasequoia* in all major morphological features. Its leaves are arranged on determinate short shoots with fascicled scale leaves at the base, as in modern *Metasequoia*. Pollen cones are axillary on specialized fertile branches, subtended by single bract, as in living *Metasequoia*. In contrast, *Sequoia* and *Sequoiadendron* produce pollen cones terminally (or subterminally) on vegetative shoots. Additionally, in both fossil and extant *Metasequoia* the seed cones have decussate cone scales, while the sister clade comprised of *Sequoia* and *Sequoiadendron* have cones with helically arranged scales as in other members of early-diverging Cupressaceae.

9. *Taxodium* – *Glyptostrobus* divergence

Fossils: *Taxodium wallissii* from the Horseshoe Canyon Formation, Alberta (45). These deposits are dated to the Maastrichtian (70-65 My).

Prior: Lognormal; 65-85 (105) My (95% confidence intervals)

Discussion: *Taxodium wallissii* is a whole plant reconstruction that is similar to modern *Taxodium* in all major morphological features. Pollen cones were produced in axillary clusters on branches (which also terminate in a cone), similar to the fertile branches in extant *Taxodium*. In contrast, *Glyptostrobus* (sister genus to *Taxodium*) has pollen cones that are borne terminally on vegetative shoots. *Taxodium wallissii* is also similar to modern *Taxodium* in its seeds, which are unwinged and prominently three angled; a morphology that is unique to *Taxodium* among living conifers.

10. *Papuacedrus* – (other Callitroids) divergence

Fossils: *Papuacedrus prechilensis* from the Laguna del Hunco and Rio Pichileufu floras, Argentina (46), radiometrically dated to the Early to Middle Eocene (51.9-47.5 My).

Prior: Lognormal; 51.9-71.9 (91.9) My (95% confidence interval)

Discussion: *Papuacedrus prechilensis* has leafy shoots bearing foliage indistinguishable from the characteristic dimorphic transitional foliage of extant *Papuacedrus*. The foliage leaves also have stomata in separate rows that are not confined to medial strips, which is also characteristic of *Papuacedrus* to the exclusion of related genera such as *Austrocedrus* and *Libocedrus*. The seed cone of *P. prechilensis* is also similar to extant *Papuacedrus*, with two pairs of highly dimorphic valvate scales. Characteristically, the bract apex is at the center of a long shield-like scale. Among related genera, *Libocedrus* has a much longer pointed bract apex and the apex of *Austrocedrus* is at the margin of the scale.

11. *Thuja – Thujopsis* divergence

Fossils: *Thuja polaris* from the Strand Bay Formation - Iceberg Bay Formation of the Eureka Sound Group on Ellesmere Island, dated to the Middle Paleocene (47).

Prior: Lognormal; 58-78 (98) My (95% confidence intervals)

Discussion: *Thuja polaris* has leaflets that are broad and flattened in regular splays, unlike closely related *Thujopsis* which has similar, but irregular splays. Cones of *T. polaris* are similar to those of extant *Thuja* in having long thin scales with reflexed umbos, and a central columella-like structure formed from two connate apical scales. In contrast, *Thujopsis* cones scales are more robust and lack the columella-like structure. We therefore interpret *T. polaris* as evidence for a minimum age of the *Thuja*-*Thujopsis* divergence.

12. *Tetraclinis* – (*Platycladus*+*Microbiota*) divergence

Fossils: *Tetraclinis salicornoides* from the Lost Creek Locality of the Bridge Creek Flora (48), which is considered to be early Oligocene in age (28-33 My; 49).

Prior: Lognormal; 28-48 (68) My (95% confidence intervals)

Discussion: *Tetraclinis salicornoides* is known from fossil foliage, seeds, and seed cones. Its seed cones are extremely similar to extant *Tetraclinis*, and have two pairs of dimorphic, valvate scales with cordate bases. Fossil seeds also have large symmetric wings, similar to living *Tetraclinis*. *Tetraclinis* foliage (*T. brachyodon*) is described from European sediments as far back as the Eocene, although floras with preserved cones are not known until the Oligocene (48). We therefore conservatively consider the Oligocene to be the earliest unambiguous appearance for the stem group of extant *Tetraclinis*.

13. *Juniperus – Cupressus* sensu lato divergence

Fossils: *Juniperus pauli* from the Ústí Formation, Czech Republic, dated to the Eocene/Oligocene boundary (~33 My; 50).

Prior: Lognormal; 33-53 (73) My (95% confidence intervals)

Discussion: *Juniperus pauli* has the characteristic fibrous spherical cones and the relatively large, wingless seeds with resin scars that are typical of extant *Juniperus*. Kvaček (50) assigns *J. paulii* to extant section *Sabina* based on its cuticular characters, which include weakly cutinized Florin rings and indistinct or absent distal papillae on the adaxial leaf side. However, a more comprehensive analysis of the evolution of cuticular features *Juniperus* would be necessary in order to determine whether they can be used to place this fossil within crown *Juniperus*, or whether it represents a stem member. We therefore consider this fossil as unambiguous evidence of *Juniperus*, but do not place it within crown *Juniperus* or use it to date sectional splits within the genus.

14. *Picea*- *Cathaya* divergence

Fossils: *Picea burtonii* from the Apple Bay locality, Vancouver Island, British Columbia (51), dated to the Valanginian Stage of the Early Cretaceous (~140-133 My)

Prior: Lognormal; 133-153 (173) My (95% confidence intervals)

Discussion: This seed cone specimen shares a number of morphological and anatomical characteristics with extant *Picea*, especially in regards to the precise distribution and branching pattern of resin canals in the ovule scale. A cladistic analysis including fossil and living seed cone specimens resolved this fossil as more closely related to extant *Picea* than *Cathaya* (51), leading the authors to suggest that this fossil can be used to date the divergence of these two lineages. Based on their analysis, we follow this interpretation.

15. *Larix – Pseudotsuga* divergence

Fossils: *Larix altoborealis* from the Buchanan Lake formation, Axel Heiberg Island (52), dated to the Middle Eocene (41-47 My).

Prior: Lognormal; 41-61 (81) My (95% confidence intervals)

Discussion: Fossil *Larix altoborealis* is known from foliage, shoots, and attached seed cones that are virtually identical to modern *Larix*. As in extant species in the genus, *L. altoborealis* branches have short shoots bearing leaves and upright cones. Closely related *Pseudotsuga* does not produce short shoots and has ovulate scales with much longer bracts.

16. *Tsuga – Nothotsuga* divergence

Fossils: *Tsuga swedaea* from the Buchanan Lake formation, Axel Heiberg Island (53), dated to the Middle Eocene (41-47 My).

Prior: Lognormal; 41-100 My (95% confidence intervals)

Discussion: *Tsuga swedaea* is known from well-preserved mummified seed cones. These seed cones are not distinguishable from *Nothotsuga* based on morphology, since both taxa have numerous scales and well-developed bracts. However, non-saccate pollen similar to extant *Tsuga canadensis* is known from this formation (53). Since *Nothotsuga* pollen has more developed sacci than most *Tsuga* species (except *T. mertensiana*), the presence of *Tsuga*-like pollen suggests that the split between *Nothotsuga* and *Tsuga* had occurred by the Middle Eocene. This pollen morphology (*Tsugapollenites*) is also known earlier in the fossil record, from Paleocene and perhaps even Late Cretaceous deposits (see summary in 53). These records suggest *Tsuga* may have a deeper history, but these grains are not associated with any diagnostic foliar or cone macrofossils and we therefore regard them as insufficient for an unambiguous indicator of the presence of *Tsuga* clade. Therefore, we use *T. swedaea* to set the minimum age for the calibration, but extend the 95% confidence intervals of the prior age distribution to the beginning of the Late Cretaceous (~100 My) to include Late Cretaceous *Tsuga*-like pollen grains that may have been produced by members of the *Tsuga* lineage.

Fossils not used in our analyses

In this section, we discuss fossils that were initially considered for their potential to date divergences within conifers but were ultimately not used. Generally, these fossils were excluded because we felt there was too much uncertainty regarding their phylogenetic placement, particularly in terms of whether or not the fossil taxa represented stem or crown members of the clades of interest. However, these fossils merit discussion because many have been used in previous analyses to date divergences, or because they could be particularly useful for dating divergences if more were known about them or their systematic placement. The use of these fossils may result in older divergence time estimates in some cases, because they often represent ambiguous early occurrences of clades or particular traits. This is not universally true, however; the first unambiguous fossil appearance of cone morphology indicative of Cupressaceae *sensu stricto* (*Widdringtonia americana* at ~95 My; 54) postdates the estimated divergence time for the clade when this fossil information is not used in the analysis.

Wollemia-like foliage and pollen

Fossils: *Dilwynites* pollen is known from the Turonian of Australia (89-93 My) and leaves very similar to modern *Wollemia* are known from the Cenomanian (93-99 My) Winton flora from Queensland (55).

Potential calibration node: *Wollemia – Agathis* divergence

Discussion: Fossil *Dilwynites* pollen is similar to that of modern *Wollemia* in the thickness of the exine and the pronounced granular ornamentation, whereas modern *Araucaria* and *Agathis* pollen have a thinner exine and a less granular surface. While some fossil leaves assigned to *Wollemia* are very similar to the extant genus, they show a range of variation that exceeds that of extant *Wollemia*. The seed cone scales of both *Agathis* and *Wollemia* are somewhat similar in their lack of a ligule, making the assignment of associated ovulate scales to either lineage difficult. The Winton flora also contains *Wollemia*-like pollen cones, although these are also not diagnostic for the genus. Given the uncertainties in the interpretation of these fossils and their disarticulated nature, it is not unambiguously clear whether they represent crown members of the *Wollemia – Agathis* clade or stem members predating the divergence between the extant genera. While the pollen evidence is suggestive that the *Wollemia* lineage had diverged by the Turonian, we decided not to base a calibration point on this evidence because the systematic and taxonomic importance of the characters in which *Wollemia* and other Araucariaceae differ are not clear.

Notophytum krauselii

Fossils: Stems and attached leaves from the Fremouw Formation, Antartica (56), which is dated to the Early Middle Triassic (Anisian; 241-245 My)

Potential calibration node: Podocarpaceae-Araucariaceae divergence

Discussion: *Notophytum krauselii* consists of multiveined leaves attached to stems that are referred Podocarpaceae on the basis of the abundant sclereids, the position of transfusion tissue, and the presence of resin canals below the vascular bundle. Large multi-vein leaves of this kind are characteristic of some extant Podocarpaceae (as well as *Agathis* in the Araucariaceae), and this fossil has been used to date the Podocarpaceae - Araucariaceae divergence (57). However, among extant Podocarpaceae multi-vein leaves are characteristic of derived taxa with a relatively recent divergence (*Nageia*; see 58) and their presence in Early Triassic members seems unlikely. Furthermore, recent studies have linked *Notophytum* foliage with *Parasciadopitys* cones (58), which are not similar morphologically to known members of Podocarpaceae. *Notophytum* foliage may represent the permineralized form of *Heidiphyllum* compression foliage, a widespread Gondwanan leaf that is associated with a compression seed cone (*Telemachus*) also unlike modern Podocarpaceae (58). *Notophytum* fossils therefore may belong to an extinct conifer group whose relationships have not been currently resolved. We therefore did not use these fossils to calibrate the Podocarpaceae – Araucariaceae split.

Rissikia plant

Fossils: Leafs, shoots, and associated ovulate and pollen cones from the Late Triassic (Carnian; 228-235 My) Molteno Formation in South Africa (59, 60)

Potential calibration prior: Podocarpaceae – Araucariaceae divergence

Discussion: The reconstructed *Rissikia* plant consists of several species that include associated foliage (*Rissikia*), pollen cones (*Rissikianthus*), and ovulate cones (*Rissikistrobus*) that are believed to belong to the same living plant based on shared cuticular features, attachment, and association evidence. Taken separately, any particular feature or organ is not diagnostic of Podocarpaceae, but the plant has been assigned to the family when considered as a whole.

Rissikia leaves are similar to some extant Podocarpaceae in that they are single veined, bifacially flattened, and rotated into a plane, although some other conifer groups such as Taxaceae also show these features. *Rissikia* foliage also has a short shoot/long shoot arrangement that is similar to the extant Podocarpaceae genera *Acmopyle* and *Dacrycarpus*. *Rissikianthus* pollen cones are attached to branches with scale leaves and have two unfused microsporangia containing bisaccate pollen grains. This is morphology is similar to extant Podocarpaceae, although these features are not strictly diagnostic of the family. Several living and extinct conifer groups produce bisaccate pollen and have pollen cones with two microsporangia per microsporophyll. The pollen grains themselves are also faintly striate, a feature not seen in any extant group of conifers.

The ovulate cone structure is significantly different than that of extant Podocarpaceae. Townrow (59) interpreted the ovules are being covered by an epimatium, but based on the figured specimens the evidence for this structure is not completely clear. The basic unit of the *Rissikia* cones consists of two ovules borne on a small scale that is subtended by subtended unfused bract; these units are then often clustered groups of three which are helically arranged around an axis. Since these ovulate cones are very different from modern Podocarpaceae (as well as extant Araucariaceae and extant conifers in general) we do not consider these fossils to represent unambiguous evidence of the appearance of Podocarpaceae by the Late Triassic.

Parasciadopitys aequata

Fossils: Permineralized cone from Fremouw Formation, Antartica (61), which is dated to the Early Middle Triassic (Anisian; 241-245 My)

Potential calibration node: Cupressaceae sensu lato – Taxaceae divergence

Discussion: *Parasciadopitys aequata* was originally assigned to the Cupressaceae *sensu lato* ("Taxodiaceae") based on its general similarity in morphology and vasculature to *Sciadopitys* (which was considered to be included in Cupressaceae *sensu lato* at the time). However, the cone is not readily distinguishable from other fossil ovulate cones considered to belong to the more primitive voltzialean conifer group – such as *Aethophyllum*, *Telemachus*, and *Swedenborgia*. More recent work (58) compares *Parasciadopitys* cones to those of *Telemachus*, which was previously considered to be an early member of Podocarpaceae. This suggests these fossils may belong to an extinct group with combinations of features seen in several different extant groups. For example, *Parasciadopitys* and *Telemachus*, that have ovule scales comparable to those of Cupressaceae, are associated with multiveined "podocarpaceous" leaves (*Notophytum* and *Heidiphyllum* respectively; see above discussion of *Notophytum*). Without additional evidence from pollen or pollen cones we cannot assign these species definitively to Cupressaceae.

Widdringtonia americana

Fossils: *Widdringtonia americana* from the Tuscaloosa Formation in Alabama (54), dated to the Cenomanian (~95 My).

Prior: Cupressaceae *sensu stricto* – Taxodioid clade of Cupressaceae *sensu lato* divergence

Discussion: McIver (54) assigns leafy shoots and attached cones to extant *Widdringtonia* based on overall similarity in the seed cones. While it is true that the fossil has 4 decussate, valvate cone scales as in extant *Widdringtonia*, this is also seen in several unrelated genera of Cupressaceae, including *Callitropsis*, *Diselma*, and *Tetraclinis*. In addition, the fossil cones of *W. americana* do appear more similar to *Widdringtonia* than other extant genera, but they are significantly smaller than living species and also lack their characteristic warty protuberances. Molecular evidence from this and other studies also suggests *Widdringtonia* is a relatively recently derived genus nested within the callitroid clade and the modern geographical range in southern Africa, where there are four species, is far removed from these North American localities. Together, the lack of diagnostic synapomorphies, the disjunction in geographical range between fossil and living species, and the much greater age for the Cupressaceae as a whole implied by a derived taxon such as *Widdringtonia* appearing at 95 My, suggests this fossil may not belong to the modern genus. However, its decussate scale leaves and 4-valved cone do provide strong evidence of a conifer that clearly belongs within the lineage of extant Cupressaceae *sensu stricto*. However, in light of the older age for the Cupressaceae *sensu stricto* found by Mao *et al.* (62) compared to our initial analyses in which we used *W. americana* to calibrate this divergence, we chose not to use this calibration point in order to more directly compare results between the two studies.

Chamaecyparis corpulenta

Fossils: Leafy shoots with attached seed cones from the Late Cretaceous (Santonian; 83-85 My) Comox Formation, Vancouver Island, British Columbia (63)

Potential calibration node: *Chamaecyparis – Fokienia* divergence

Discussion: *Chamaecyparis corpulenta* was assigned to extant *Chamaecyparis* based on very small, spherical seed cones with pairs of peltate, interlocking decussate scales. However, seed cones of modern *Chamaecyparis* species have more than the four scales present in these fossils. Although extremely small seed cones are unique to *Chamaecyparis* among extant Cupressaceae, the architecture of the leafy shoots of this fossil species differs from that of extant *Chamaecyparis* (or any other Northern Hemisphere species of Cupressaceae) in that is has both alternate and opposite branches. Opposite branching is seen today only in some Southern Hemisphere genera such as *Papuacedrus*. This difference in branching architecture raises the possibility that *C. corpulenta* is not within the crown *Chamaecyparis–Fokienia* clade, although the importance of opposite versus alternate branching as a phylogenetic character in Cupressaceae requires more study. Because of the uncertainties regarding the diagnostic value of the foliage characters and because *C. corpulenta* also lacks strongly diagnostic seed cone features (other than its small size), further studies are needed before the relationships of this species to extant *Chamaecyparis* can be demonstrated securely.

Fokienia ravenscragensis

Fossils: Leafy shoots with attached seed cones from the Early Paleocene (65.5-61.7 My) Ravenscrag Formation, Saskatchewan, Canada (64).

Potential calibration node: *Chamaecyparis – Fokienia*

Discussion: Fossil *Fokienia ravenscragensis* was assigned to extant *Fokienia* based on the structure of their ovulate seed cones, which are similar to those of the extant genus although they are smaller and bear fewer scales. As is also true of *Chamaecyparis corpulenta*, the opposite branching of this species also differs from extant *Fokienia* and other Northern Hemisphere Cupressaceae. While the ovulate cones of *F. ravenscragensis* are similar to those of *Fokienia*, they are also generally similar to seed cones of many Cupressaceae and lack strongly diagnostic features. Some phylogenetic analyses (although not those conducted in this study) suggest extant *Fokienia* is nested within *Chamaecyparis*, and therefore that this fossil (in conjunction with *Chamaecyparis corpulenta*) could be used to date the presence of crown *Chamaecyparis* in the fossil record (as in 62). However, given the lack of unique diagnostic features in *Fokienia ravenscragensis*, their relatively small size compared to those of modern taxa, and the differences in branching between the fossils and living taxa, we think it is premature to use *F. ravenscragensis* to calibrate the *Fokienia-Chamaecyparis* split until more is known about it.

Pseudolarix erensis

Fossils: Shoots and cone scales from Mongolia, dated to the Late Jurassic or Early Cretaceous (65)

Potential calibration node*: Pseudolarix – Tsuga* divergence

Discussion: This fossil material includes short shoots, leaves, and scales that appear similar to extant *Pseudolarix* (65, 66). They were also used by Gernandt et al. (67) as one of two potential calibration schemes for the first appearance of the Pinaceae. However, the stratigraphy, and therefore the dating, of these localities is not clear. Krassilov (65) thought they were similar in age to the Tsagan Tsab Formation, which he considered Early Cretaceous but which has been radiometrically dated to the Oxfordian, ~156 My at some localities (68). However, Krassilov provides no direct evidence that that deposits containing *Pseudolarix* are coeval with the Tsagan Tsab. These deposits also contain apparent angiosperm seeds and foliage, raising further questions about a Late Jurassic date for these deposits. Therefore, these fossils were not used in the analysis even though their morphology suggests they are similar to extant *Pseudolarix*.

Pinus belgica

Fossils: Permineralized seed cone, probably from the Early Cretaceous (145-89 My) Wealden Formation, Belgium (69)

Potential calibration node: *Pinus* – (*Picea*+*Cathaya*) divergence

Discussion: The morphology and anatomy of this specimen unambiguously places it within *Pinus*. However, its provenance is uncertain and it is attributed to the Wealden Formation based on adhering particles and its general type of preservation (69). This is especially problematic because the Belgian Wealden has a wide range of possible dates, spanning 127-89 My (67, 70). It is therefore possible that this cone is actually similar in age to the first appearance of *Pinus* that is well placed stratigraphically – *Pinus mutoi* in the Coniacian (71). Due to the uncertainties in the provenance of the cone and its age, it was not used in the analyses.

Pinus hokkaidoensis

Fossils: Permineralized needles from the Upper Yezo Group, Hokkaido (72) dated to the Late Cretaceous (Santonian, 83-85 My).

Potential calibration node: *Pinus* Subsection *Strobus* – *Pinus* Subsection *Pinus* divergence

Discussion: *Pinus hokkaidoensis* possesses needles with two vascular strands, a feature unique to *Pinus* Subsection *Pinus* among extant Pinaceae, and could be used to indicate divergence of the two major *Pinus* subsections had occurred by the Late Cretaceous. In addition to this fossil, needles with two vascular bundles are known from Santonian-Coniacian of Massachusetts (73) and wood with features indicative of *Pinus* subsection *Strobus* (nondentate ray tracheids) also occurs by the Santonian (74). However, in the Eocene Princeton Chert, cones of *Pinus arnoldii* show with a mixture of Subsection *Pinus* characters (pronounced umbos, inflated scales, and sclerified outer cortex in the cone axis) and Subsection *Strobus* characters (cylindrical cones). These cones are strongly associated with single-bundled needles, suggesting to Miller (75) that the *Pinus*/*Strobus* divergence had not occurred by the Eocene. More recently, the *P. arnoldii* plant has been fully reconstructed (76), further strengthening the relationship between subsection *Pinus*-like cones and *Strobus*-like leaves. Because the fossil evidence does not resolve when the split between these groups occurred, and because fossil taxa exist with intermediate character combinations, *Pinus hokkaidoensis* was not used to calibrate the *Pinus*/*Strobus* split.

Abies deweyensis

Fossils: Twigs and seeds from the Thunder Mountain Flora, Idaho (77), radiometrically dated to the Middle Eocene (45.5 My).

Potential calibration node: *Abies – Keteleeria* divergence

Discussion: *Abies deweyensis* twigs are similar to extant *Abies* in their characteristic circular leaf scars and leaves with expanded bases, although circular leaf scars are also found in closely related extant *Keteleeria*. Seeds present in the Thunder Mountain Flora are also similar to extant *Abies*, in the slight marginal lobe of the seed wing where it connects to the seed. This material was used by Gernandt *et al*. (67) to date the *Abies* divergence. However, given the fragmentary nature of the material generally and the lack of articulated cones we do not use it to date this split.

References

1. de Laubenfels DJ (1988) Coniferales. Flora Malesiana, Series I, Vol. 10 (Kluwer Academic Press, Dordrecht), pp. 337-453.

2. Farjon A (1990) *Pinaceae* (Koeltz Scientific Books, Germany, 1990).

3. Farjon, A (2005) *A Monograph of Cupressaceae and Sciadopitys* (Royal Botanic Gardens, Kew, UK).

4. Eckenwalder JE (2009) *Conifers of the World* (Timber Press, Portland, USA).

5. Conran JG *et al*. (2000) Generic relationships within and between the gymnosperm families Podocarpaceae and Phyllocladaceae based on an analysis of the chloroplast gene *rbc*L. *Aust J Bot* 48: 715-724.

6. Gradstein F, *et al*. (2004) A Geologic Time Scale 2004. (Cambridge University Press, Cambridge, UK).

7. Morlon H, Potts MD, Plotkin JB (2010) Inferring the dynamics of diversification: a coalescent approach. *PloS Biology* 8: e1000493.

8. Burnham KP, Anderson DR (2012) Model Selection and Multimodel Inference, 2nd Edition (Springer-Verlag, New York).

9. Gao Z, Thomas BA (1989) A review of fossil cycad megasporophylls, with new evidence of *Crossozamia* Pomel and its associated leaves from the Lower Permian of Taiyuan, China. *Rev Palaeobot Palyno* 60: 205-223.

10. Rothwell GW, Scott AC (1992) *Stamnostoma oliveri*, a gymnosperm with systems of ovulate cupules from the Lower Carboniferous (Dinantian) floras at Oxroad Bay, East Lothian, Scotland. *Rev Palaeobot Palyno* 72: 273-284.

11. Stewart WN, Rothwell GW (1993) Paleobotany and the Evolution of Plants, 2nd Edition (Cambridge University Press, Cambridge).

12. Mapes G, Rothwell GW (1980) *Quaestora amplecta* gen. et sp. n., a structurally simple medullosan stem from the Upper Mississippian of Arkansas. *Am J Bot* 67: 636-647.

13. Rothwell GW, Serbet R (1994) Lignophyte phylogeny and the evolution of spermatophytes: a numerical cladistic analysis. *Syst Bot* 19: 443-482.

14. Doyle JA (2006) Seed ferns and the origin of angiosperms. *J Torrey Bot Soc* 133: 169-209.

15. Hilton J, and Bateman RM (2006) Pteridosperms are the backbone of seed-plant phylogeny. *J Torrey Bot Soc* 133: 119-168.

16. Clayton G (1996) *Palynology: principles and applications*, Vol. 2, eds. Jansonius J, McGregor DC (American Association of Stratigraphic Palynologists Foundation), pp. 589-596.

17. Zhou Y-X (1994) Earliest pollen-dominated microfloras from the early Late Carboniferous of the Tian Shan Mountains, NW China: their significance for the origin of conifers and palaeophytogeography. *Rev Palaeobot Palyno* 81: 193-211.

18. Crisp MD, Cook LG (2011) Cenozoic extinctions account for the low diversity of extant gymnosperms compared with angiosperms. *New Phytol* 192: 997-1009.

19. Axsmith BJ, Ash SR (2006) Two rare fossil cones from the Upper Triassic Chinle Formation in Petrified Forest National Park, Arizona, and New Mexico. *Mus N Ariz Bull* 62: 82-94.

20. Harris TM (1979) The Yorkshire Jurassic Flora. V. Coniferales. (British Museum of Natural History, London).

21. Archangelsky S, Del Fueyo GM (1989) *Squamastrobus* gen. n., a fertile podocarp from the early Cretaceous of Patagonia, Argentina. *Rev Palaeobot Palyno* 59: 109-126.

22. de Jersey N (1968) Triassic spores and pollen grains from the Clematis Sandstone. *Geol Surv Queensland Austr Publ No. 338, Palaeont Pap* 14: 1-44.

23. Ottone EG, Mancuso AC, Resano M (2005) Miospores and chlorococcalean algae from the Los Rastros Formation, Middle to Upper Triassic of central-western Argentina. *Ameghiniana* 42: 347-362.

24. Pederson KR, Lund JJ (1980) Palynology of the plant-bearing Rhaetian to Hettangian Kap Stewart Formation, Scoresby Sund, East Greenland. *Rev Palaeobot Palyno* 31: 1-69.

25. Harris TM (1935) The fossil flora of Scoresby Sound East Greenland. Part 4: Ginkgoales, Coniferales, Lycopodiales, and isolated fructifications. Medd, Grønland 112: 1-176.

26. Lele KM (1956) Plant fossils from the Parsora in the South Rewa Gondwana Basin, India. *Palaeobotanist* 4: 23-34.

27. Litwin RJ, Traverse A, Ash SR (1991) Preliminary palynological zonation of the Chinle Formation, southwestern U.S.A., and its correlation to the Newark Supergroup (eastern U.S.A.). *Rev Palaeobot Palyno* 68: 269-287.

28. Riggs NR, Ash SR, Barth AP, Gehrels GE, Wooden JL (2003) Isotopic age of the Black Forest Bed, Petrified Forest Member, Chinle Formation, Arizona: an example of dating a continental sandstone. *GSA Bull* 115: 1315-1323.

29. van Konijnenburg-van Cittert JHA (1971) *In situ* gymnosperm pollen from the Middle Jurassic of Yorkshire. *Acta Bot Neerl* 20: 1-97.

30. Stockey RA (1994) Mesozoic Araucariaceae: morphology and systematic relationships. *J Plant Res* 107: 493-502.

31. Stockey RA (1980) Anatomy and morphology of *Araucaria sphaerocarpa* Carruthers from the Jurassic Inferior Oolite of Bruton, Somerset. *Bot Gaz* 141: 116-124.

32. Page KN (1996) Observations on the succession of stratigraphically useful ammonite faunas in the Bathonian (Middle Jurassic) of south-west England, and their correlation with a Sub-Mediterranean 'Standard Zonation'. *Proc Ussher* 9: 45-53.

33. Fenton JPG, Neves R, Piel KM (1980) Dinoflagellate cysts and acritarchs from Upper Bojocian to Middle Bathonian strata of central and southern England. *Palaeontology* 23: 151-170.

34. Stockey RA (1975) Seeds and embryos of *Araucaria mirabilis*. *Am J Bot* 62: 856-868.

35. Falaschi P, Grosfeld J, Zamuner AB, Foix N, Rivera SM (2011) Growth Architecture and silhouette of Jurassic conifers from La Matilde Formation, Patagonia, Argentina. *Palaeogeogr Palaeoecol* 302: 122-141.

36. Wilf P (2012) Rainforest conifers of Eocene Patagonia: attached cones and foliage of the extant Southeast-asian and Australasian genus *Dacrycarpus* (Podocarpaceae). *Am J Bot* 99: 562-584.

37. Hill RS (1989) New species of *Phyllocladus* (Podocarpaceae) macrofossils from south eastern Australia. *Alcheringa* 13: 193-208.

38. Hill RS, Brodribb TJ (1999) Southern conifers in time and space. *Aust J Bot* 47: 639-696.

39. Hill RS, Merrifield HE (1993) An early Tertiary macroflora from West Dale, southwestern Australia. *Alcheringa* 17: 285-326.

40. Florin R (1958) On Jurassic taxads and conifers from north-western Europe and Eastern Greenland. *Acta Horti Bergiani* 17: 257-402.

41. Florin R (1938-1945) Die Koniferen des Oberkarbons und des unteren Perms. I-VII. *Palaeontogr Abt B* 85:1-729.

42. Hao DC, Xiao PG, Huang B-L, Ge GB, Yang L (2008) Interspecific relationships and origins of Taxaceae and Cephalotaxaceae revealed by Bayesian analyses of chloroplast and nuclear DNA sequences. *Plant Syst Evol* 276: 89-104.

43. Liu Y-J, Li C-S, Wang Y-F (1999) Studies of fossil *Metasequoia* from north-east China and their taxonomic implications. *Bot J Linn Soc* 130: 267-297.

44. Manchester SR, Crane PR, Golovneva LB (1999) An extinct genus with affinities to extant *Davidia* and *Camptotheca* (Cornales) from the Paleocene of North America and Eastern Asia. *Int J Plant Sci* 160: 188-207.

45. Aulenback KR, LePage BA (1998) *Taxodium wallissii* sp. nov.: first occurrence of *Taxodium* from the Upper Cretaceous. *Int J Plant Sci* 159: 367-390.

46. Wilf P et al. (2009) *Papuacedrus* (Cupressaceae) in Eocene Patagonia: a new fossil link to Australasian rainforests. *Am J Bot* 96: 2031-2047

47. McIver EE, Basinger JF (1989) The morphology and relationships of *Thuja polaris* sp. nov. (Cupressaceae) from the early Tertiary, Ellesmere Island, Arctic Canada. *Can J Bot* 67: 1903-1915.

48. Kvaček Z, Manchester SR, Schorn HE (2000) Cones, seeds and foliage of *Tetraclinis salicornoides* (Cupressaceae) from the Oligocene and Miocene of western North America: A geographic extension of the European Tertiary species. *Int J Plant Sci* 161: 331-344.

49. Manchester SR, Crane PR (1987) A new genus of Betulaceae from the Oligocene of western North America. *Bot Gaz* 148: 263-273.

50. Kvaček Z (2002) A new juniper from the Palaeogene of central Europe. *Feddes Repertorium* 113: 492-502.

51. Klymiuk AA, Stockey RA (*in press*) A Lower Cretaceous (Valanginian) seed cone provides the earliest fossil record for *Picea* (Pinaceae) *Am J Bot*

52. LePage BA, Basinger JF (1991) A new species of *Larix* (Pinaceae) from the early Tertiary of Axel Heiberg Island, Arctic Canada. *Rev Palaeobot Palyno* 70: 89-111.

53. LePage BA (2003) A new species of *Tsuga* (Pinaceae) from the middle Eocene of Axel Heiberg Island, Canada, and an assessment of the evolution and biogeographical history of the genus. *Bot J Linn Soc* 141: 257-296.

54. McIver EE (2001) Cretaceous *Widdringtonia* Endl. (Cupressaceae) from North America. *Int J Plant Sci* 162: 937-961.

55. Chambers TC, Drinnan AN, McLoughlin S (1998) Some morphological features of the Wollemi pine (*Wollemia nobilis*: Araucariaceae) and their comparison to Cretaceous plant fossils. *Int J Plant Sci* 159: 160-171.

56. Axsmith BJ, Taylor TN, Taylor EL (1998) Anatomically preserved leaves of the conifer *Notophytum krauselii* (Podocarpaceae) from the Triassic of Antarctica. *Am J Bot* 85: 704-713.

57. Biffin E, Brodribb TJ, Hill RS, Thomas P, Lowe AJ (2012) Leaf evolution in southern hemisphere conifers tracks the angiosperm ecological radiation. *Proc Roy Soc London* B 279: 341-348.

58. Escapa IH, Decombeix AL, Taylor EL, Taylor TN (2010) Evolution and relationships of the conifer seed cone *Telemachus*: evidence from the Triassic of Antarctica. *Int J Plant Sci* 171: 560-573.

59. Townrow JA (1967) On *Rissikia* and *Mataia* podocarpaceous conifers from the lower Mesozoic of southern lands. *Proc Roy Soc Tasmania* 101: 103-136.

60. Anderson JM, Anderson HM (2003) Heyday of the gymnosperms: systematics and biodiversity of the Late Triassic Molteno fructifications. Strelitzia 15 (National Botanical Institute, Pretoria).

61. Yao X, Taylor TN, Taylor EL (1997) A taxodiaceous seed cone from the Triassic of Antarctica. *Am J Bot* 84: 343-354.

62. Mao K *et al.* (2012) Distribution of living Cupressaceae reflects the breakup of Pangea. *P Natl Acad Sci USA* 109: 7793-7798.

63. McIver EE (1994) An early *Chamaecyparis* (Cupressaceae) from the Late Cretaceous of Vancouver Island, British Columbia, Canada. *Can J Bot* 72: 1787-1796.

64. McIver EE, Basinger JF (1990) Fossil seed cones of *Fokienia* (Cupressaceae) from the Paleocene Ravenscrag Formation of Saskatchewan, Canada. *Can J Bot* 68: 1609-1618.

65. Krassilov VA (1982) Early Cretaceous flora of Mongolia. *Palaeontogr Abt B* 181: 1-43.

66. LePage BA, Basinger JF (1995) Evolutionary history of the genus *Pseudolarix* Gordon (Pinaceae). *Int J Plant Sci* 156: 910-950.

67. Gernandt DS *et al*. (2008) Use of simultaneous analyses to guide fossil-based calibration of Pinaceae phylogeny. *Int J Plant Sci* 169: 1086-1099.

68. Keller AM, Hendrix MS (1997) Paleoclimatologic analysis of a Late Jurassic petrified forest, southeastern Mongolia. *Palaios* 12: 282-291.

69. Alvin KL (1960) Further conifers of the Pinaceae from the Wealden Formation of Belgium. *Mem Inst R Sci Nat Belg* 146: 16-21.

70. Robaszynski F, Dhondt AV, Jagt JWM (2001) Cretaceous lithostratigraphic units (Belgium). *Geol Belg* 4: 121-134.

71. Saiki K (1996) *Pinus mutoi* (Pinaceae), a new species of permineralized seed cone from the Upper Cretaceous of Hokkaido, Japan. *Am J Bot* 83: 1630-1636.

72. Stockey RA, Uedo Y (1986) Permineralized pinaceous leaves from the Upper Cretaceous of Hokkaido. *Am J Bot* 73: 1157-1162.

73. Robison CR (1977) *Pinus triphylla* and *Pinus quinquefolia* from the Upper Cretaceous of Massachusetts. *Am J Bot* 64: 726-732.

74. Meijer JJF (2000) Fossil woods from the Late Cretaceous Aachen Formation. *Rev Palaeobot Palyno* 112: 297-336.

75. Miller, CN Jr. (1973) Silicified cones and vegetative remains of *Pinus* from the Eocene of British Columbia. *Contrib Univ Mich Mus Paleontology* 24: 101-118.

76. Klymiuk AA, Stockey RA, Rothwell GW (2011) The first organismal concept for an extinct species of Pinaceae: *Pinus arnoldii* Miller. *Int J Plant Sci* 172: 294-313.

77. Erwin DM, Schorn HE (2005) Revision of the conifers from the Eocene Thunder Mountain flora, Idaho, U.S.A. *Rev Palaeobot Palyno* 137:125-145.